Modelos em bioprocessos

$$\mu_X = \frac{dX}{dt}\frac{1}{X}$$

$$Y_{X/S} = \frac{\mu_X}{\mu_S}$$

$$Y_{P/S} = \frac{\mu_P}{\mu_S}$$

Modelo de Monod

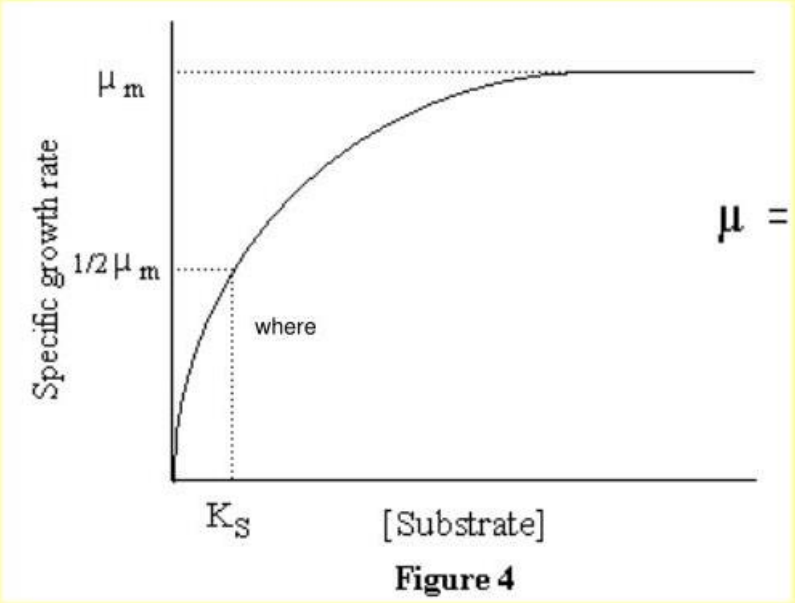

Figure 4

μ_m taxa específica de crescimento máxima
K_s constante de saturação ou de Monod
S concentração do substrato limitante .

Engenharia metabólica e Biologia de sistemas.

José Gregório Cabrera Gomez
jgcgomez@usp.br

DEPARTAMENTO DE
MICroBiologia
UNIVERSIDADE DE SÃO PAULO

Biologia e Biotecnologia

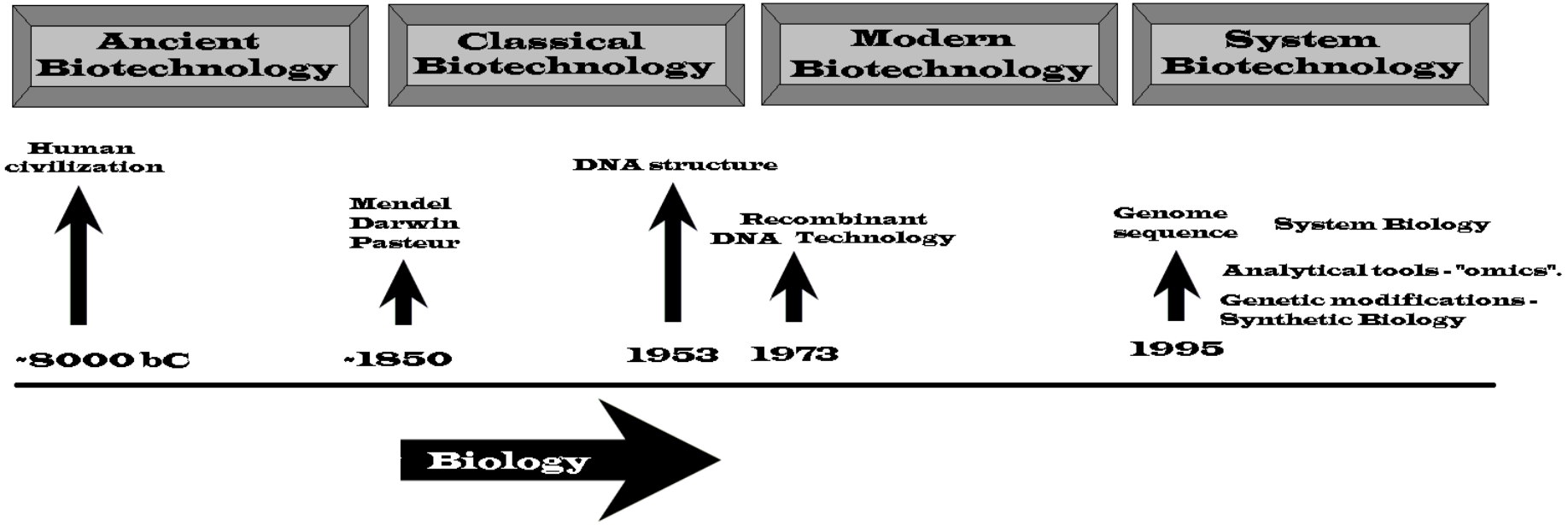

ômicas

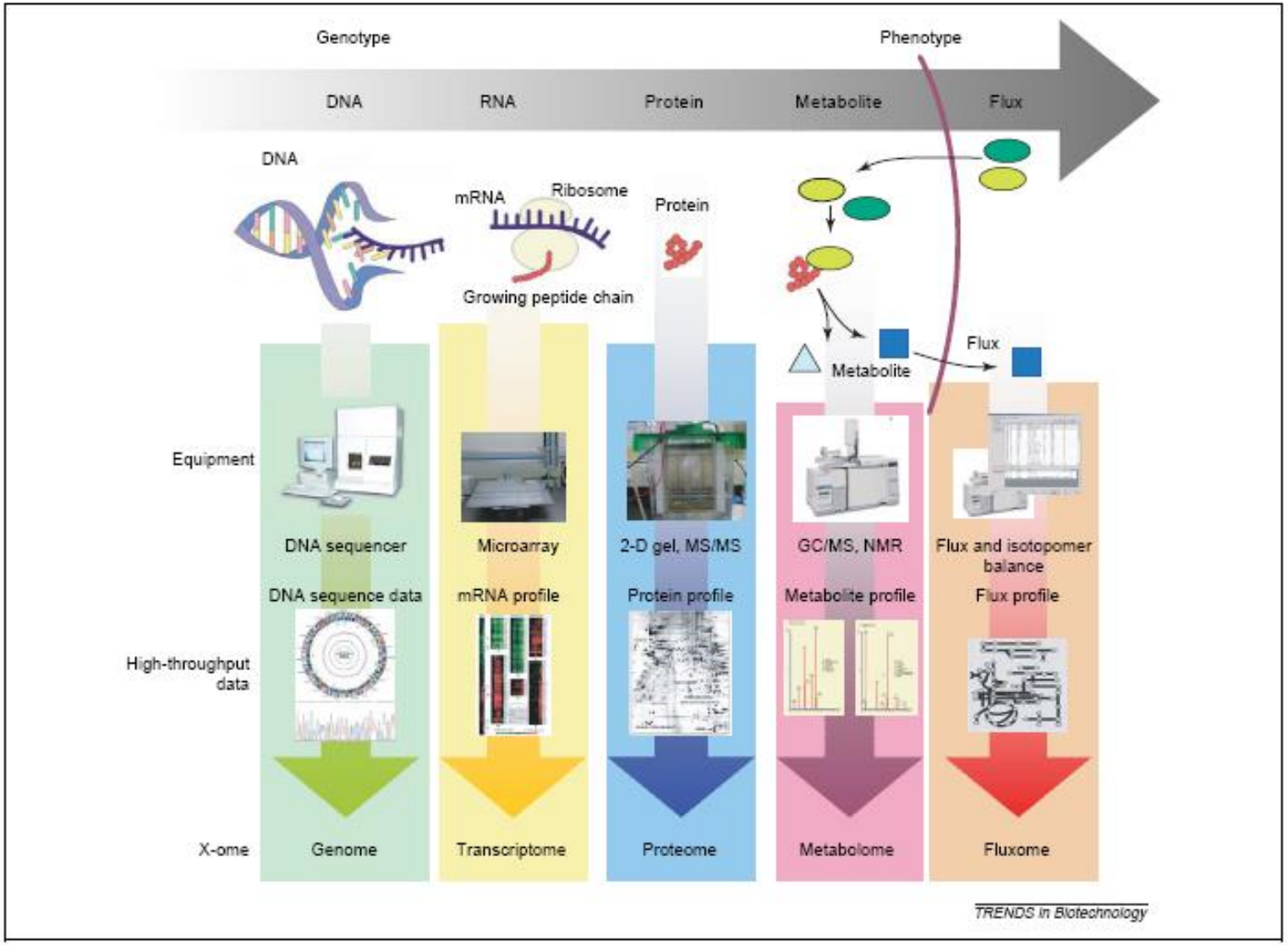

Figure 1. High-throughput omics research. Genomics advanced by the development of high-speed DNA sequencing is now accompanied by transcriptome profiling using DNA microarrays. Proteome profiling is joining the high-throughput race as 2D-gel electrophoresis combined with mass spectrography is advancing. Metabolome profiling is also rapidly advancing with the development of better GC/MS, LC/MS and NMR technologies. Isotopomer profiling followed by challenging with isotopically labeled substrate allows determination of flux profiles in the cell (fluxome).

Metabolic engineering is the improvement of cellular activities by manipulation of enzymatic, transport, and regulatory functions of the cell with the use of recombinant DNA technology. The opportunity to introduce heterologous genes and regulatory elements distinguishes metabolic engineering from traditional genetic approaches to improve strains.

... An interactive cycle of a genetic change, an analysis of the consequences, and the design of a further change...

Toward a Science of Metabolic Engineering.
James E. Bailey Science, 252: 1668-1675.

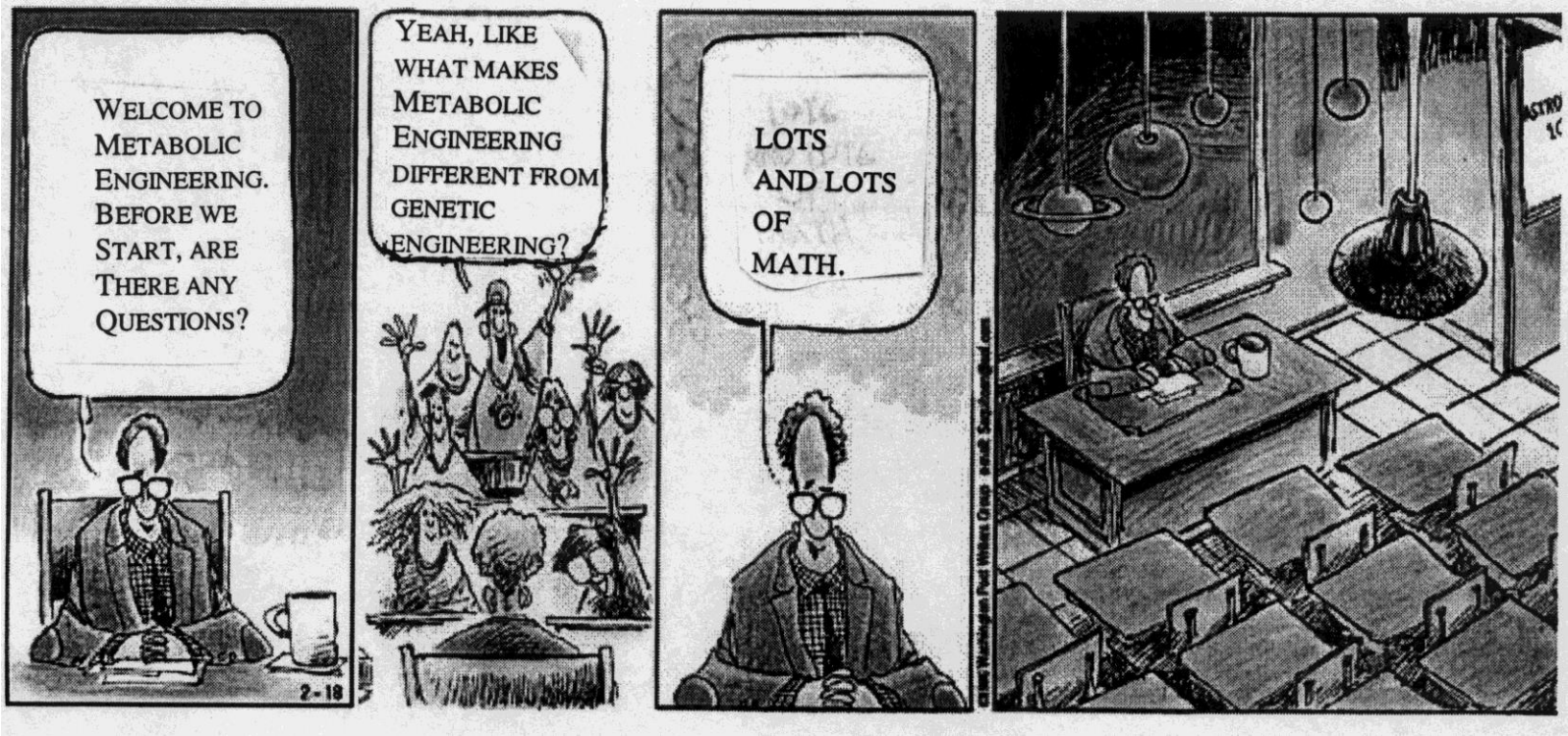

Metabolic Engineering

The knockout or overexpression of genes, usually used in Genetic Engineering, frequently does not result in product yield improvements due a resistance in the metabolism. Therefore, a better knowledge of the metabolism is needed to promote metabolism engineering as a whole to improve biotechnological processes.

Vallino & Stephanopoulos, 1992

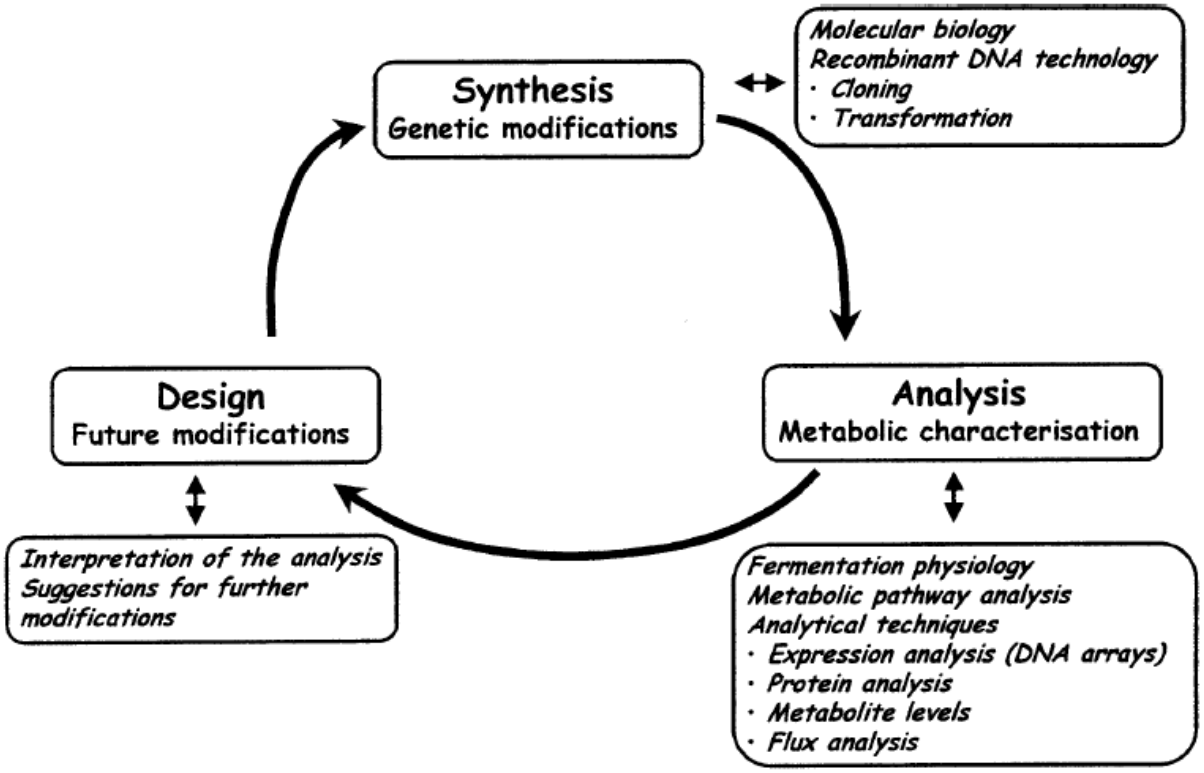

Metabolic engineering is an enabling science, and distinguishes itself from applied genetic engineering by the use of advanced analytical tools for identification of appropriate targets for genetic modifications and possibly even the use of mathematical models to perform *in silico* design of optimized cell factories. **Nielsen & Jewett, 2008 FEMS Yeast Res.**

TABLE 1. Overview of reactions, metabolites, and ORFs in reconstructed metabolic networks[a]

Organism	No. of reactions	No. of metabolites	No. of metabolic ORFs	Total no. of ORFs	% of ORFs involved in metabolism
H. pylori	444	340	268	1,638	16
H. influenzae	477	343	362	1,880	19
E. coli	720	436	695	4,485	15
S. cerevisiae	1,175	584	708	5,773	12[b]

[a] The reconstructed networks are described in references 6, 8, 17, and 18.
[b] The value is based on a recent gene count (3).

Table 3. Frequency of precursor metabolites and cofactors in a *Saccharomyces cerevisiae* genome scale model*

Precursor metabolite	No of reactions	Cofactor	No of reactions
Glucose-6P	16	ATP	188
Fructose-6P	18	ADP	146
Ribose-5P	20	NADH	65
Erythrose-4P	6	NAD^+	78
Glyceraldehyde-3P	13	NADPH	78
3-Phosphoglycerate	6	$NADP^+$	86
Phosphoenolpyruvate	12		
Pyruvate	27		
Acetyl-CoA	32		
2-Oxoglutarate	38		
Succinyl-CoA	3		
Oxaloacetate	12		

*The data are taken from the metabolic model developed by Forster *et al.* (2003).

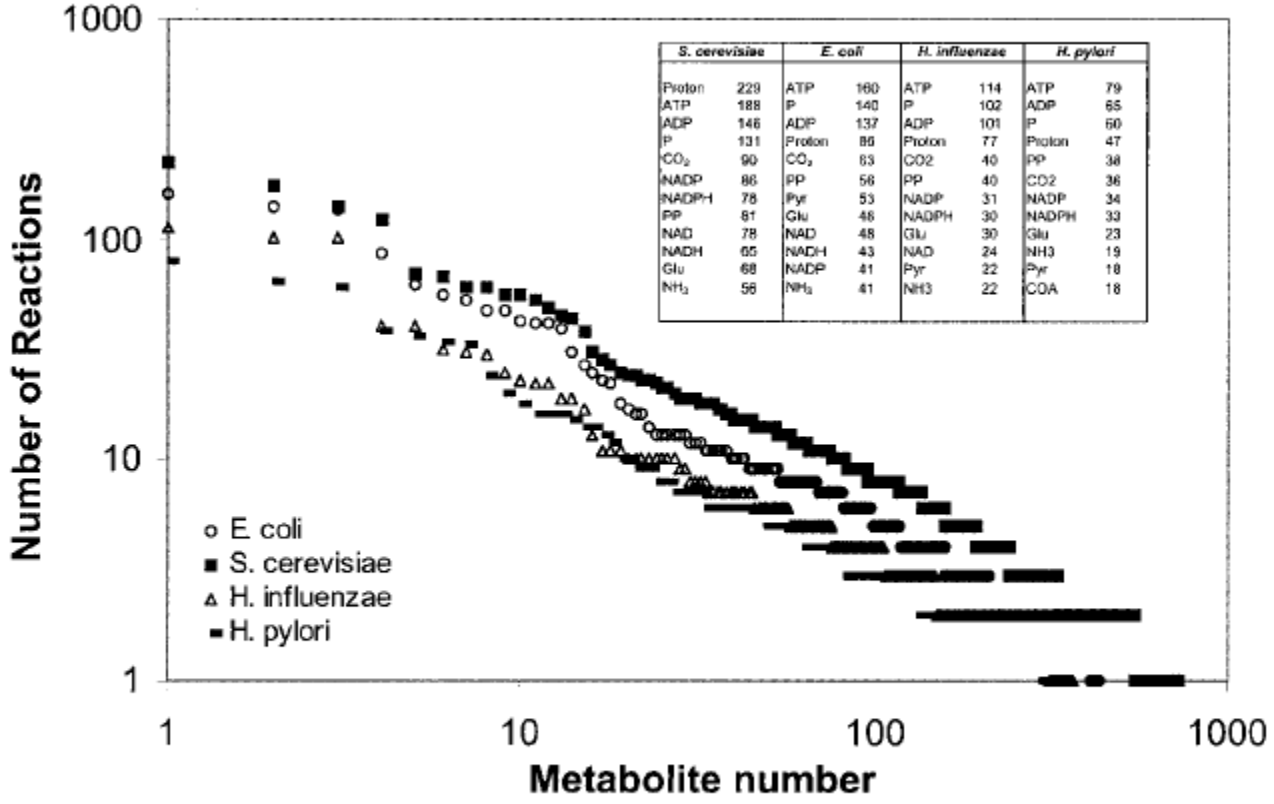

FIG. 1. Frequency plot of the number of reactions that each metabolite appears in for four different reconstructed metabolic networks. For each metabolic network the 10 metabolites that appear in the most reactions are listed. PP, pyrophosphate; COA, coenzyme A. The numbers in the box specify the numbers of reactions the 10 most frequently used metabolites participate in for the four different microorganisms.

analysis of cellular metabolism

Problem statement

Network

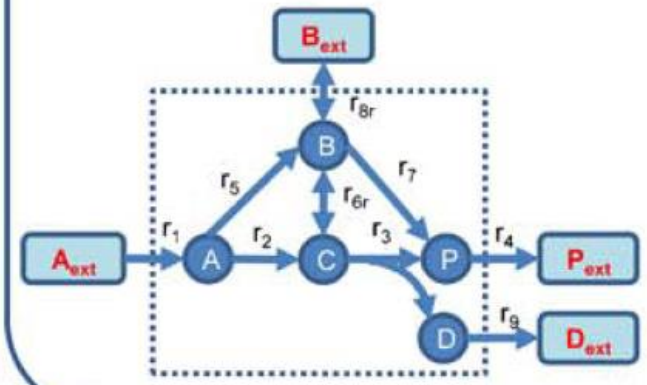

Stoichiometric reactions

r_1: $A_{ext} \rightarrow A$ r_4: $P \rightarrow P_{ext}$ r_7: $B \rightarrow 2P$
r_2: $A \rightarrow C$ r_5: $A \rightarrow B$ r_{8r}: $B \leftrightarrow B_{ext}$
r_3: $C \rightarrow P + D$ r_{6r}: $B \leftrightarrow C$ r_9: $D \rightarrow D_{ext}$

Stoichiometric matrix

$\underline{\underline{S}} =$

	r_1	r_2	r_3	r_4	r_5	r_{6r}	r_7	r_{8r}	r_9
A	1	-1	0	0	-1	0	0	0	0
B	0	0	0	0	1	-1	-1	-1	0
C	0	1	-1	0	0	1	0	0	0
D	0	0	1	0	0	0	0	0	-1
P	0	0	1	-1	0	0	2	0	0

$\underline{r} = [r_1\ r_2\ r_3\ r_4\ r_5\ r_{6r}\ r_7\ r_{8r}\ r_9]^T$

Equations to solve

$\underline{\underline{S}} \cdot \underline{r} = \underline{0}$

Thermodynamic constraints:
$r_{1\text{-}5,7,9} \geq 0$

A

$$\frac{d}{dt}\underline{C} = \underline{\underline{S}} \times \underline{r} - \mu \times \underline{C},$$

μ.C (negligible)

dC/dt = 0 (steady state)

S.r = 0 (Eq 2)

ri $\geq$ 0 (Eq 3)

Tools for analysis of cellular metabolism can be grouped into three categories, all of them developed from the same mathematical model:

(1) Metabolic flux analysis,

(2) Flux balance analysis and

(3) Metabolic pathway analysis (Elementary mode analysis).

Metabolic Flux Analysis

B

$\underline{\underline{S}}_u =$

	r_3	r_4	r_5	r_{6r}	r_7
A	0	0	-1	0	0
B	0	0	1	-1	-1
C	-1	0	0	1	0
D	1	0	0	0	0
P	1	-1	0	0	2

$\underline{\underline{S}}_m =$

	r_1	r_2	r_{8r}	r_9
A	1	-1	0	0
B	0	0	-1	0
C	0	1	0	0
D	0	0	0	-1
P	0	0	0	0

Measured fluxes

$$\underline{r}_m = \begin{bmatrix} r_1 \\ r_2 \\ r_{8r} \\ r_9 \end{bmatrix} = \begin{bmatrix} 1 \\ 0.3 \\ 0 \\ 0.75 \end{bmatrix}$$

Equations to solve

$$\underline{\underline{S}} \cdot \underline{r} = \underline{0}$$

$$\begin{bmatrix} \underline{\underline{S}}_u & \underline{\underline{S}}_m \end{bmatrix} \begin{bmatrix} \underline{r}_u \\ \underline{r}_m \end{bmatrix} = \underline{0}$$

$$\underline{r}_u = -\underline{\underline{S}}_u^{-1} \cdot \underline{\underline{S}}_m \cdot \underline{r}_m$$

Solution

$$\underline{r}_u = \begin{bmatrix} r_3 \\ r_4 \\ r_5 \\ r_{6r} \\ r_7 \end{bmatrix} = \begin{bmatrix} 0.75 \\ 1.25 \\ 0.7 \\ 0.45 \\ 0.25 \end{bmatrix}$$

A

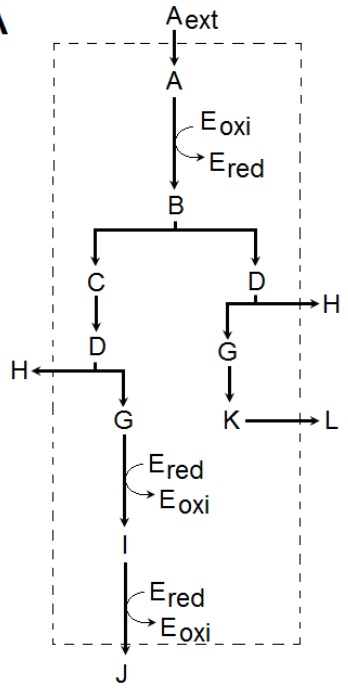

B

	r_1	r_2	r_3	r_4	r_5	r_6	r_7	r_8	r_9
Aext	-1	0	0	0	0	0	0	0	0
A	1	-1	0	0	0	0	0	0	0
B	0	1	-1	0	0	0	0	0	0
C	0	0	1	-1	0	0	0	0	0
D	0	0	1	1	-1	0	0	0	0
Eoxi	0	-1	0	0	0	1	1	0	0
Ered	0	1	0	0	0	-1	-1	0	0
G	0	0	0	0	1	-1	0	-1	0
H	0	0	0	0	1	0	0	0	0
I	0	0	0	0	0	1	-1	0	0
J	0	0	0	0	0	0	1	0	0
K	0	0	0	0	0	0	0	1	-1
L	0	0	0	0	0	0	0	0	1

C

$$\begin{bmatrix} -1 & 0 & 0 & 0 & 0 & 0 & 0 & 0 & 0 \\ 1 & -1 & 0 & 0 & 0 & 0 & 0 & 0 & 0 \\ 0 & 1 & -1 & 0 & 0 & 0 & 0 & 0 & 0 \\ 0 & 0 & 1 & -1 & 0 & 0 & 0 & 0 & 0 \\ 0 & 0 & 1 & 1 & -1 & 0 & 0 & 0 & 0 \\ 0 & -1 & 0 & 0 & 0 & 1 & 1 & 0 & 0 \\ 0 & 1 & 0 & 0 & 0 & -1 & -1 & 0 & 0 \\ 0 & 0 & 0 & 0 & 1 & -1 & 0 & -1 & 0 \\ 0 & 0 & 0 & 0 & 1 & 0 & 0 & 0 & 0 \\ 0 & 0 & 0 & 0 & 0 & 1 & -1 & 0 & 0 \\ 0 & 0 & 0 & 0 & 0 & 0 & 1 & 0 & 0 \\ 0 & 0 & 0 & 0 & 0 & 0 & 0 & 1 & -1 \\ 0 & 0 & 0 & 0 & 0 & 0 & 0 & 0 & 1 \end{bmatrix} \times \begin{bmatrix} r_1 \\ r_2 \\ r_3 \\ r_4 \\ r_5 \\ r_6 \\ r_7 \\ r_8 \\ r_9 \end{bmatrix} = \begin{bmatrix} dA/dt \\ 0 \\ 0 \\ 0 \\ 0 \\ 0 \\ 0 \\ dH/dt \\ 0 \\ dJ/dt \\ 0 \\ dL/dt \end{bmatrix}$$

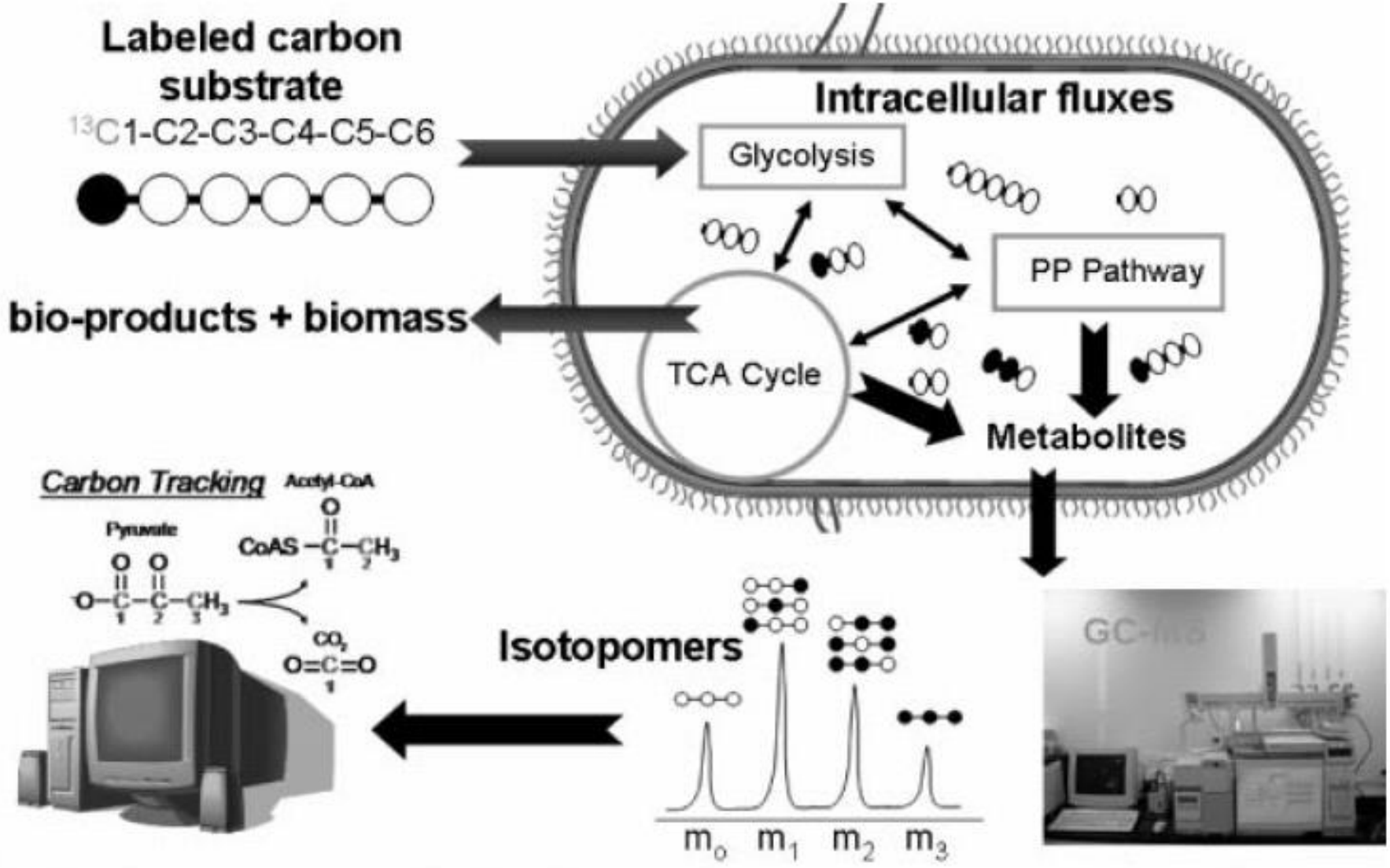

FIGURE 2. Protocol for ^{13}C-based flux analysis. [Color figure can be viewed in the online issue, which is available at www.interscience.wiley.com.]

Mass Spectrometry Reviews, **2009**, *28*, 362–375

Metabolic Engineering

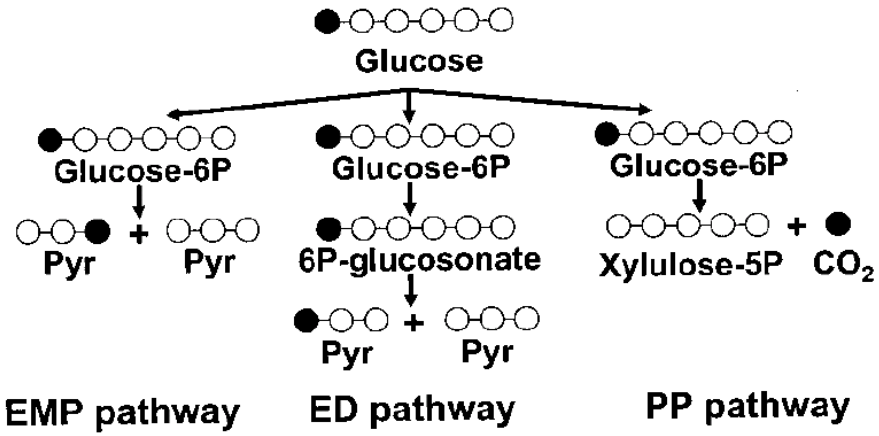

FIG. 2. Illustration of how measurement of the ^{13}C enrichment patterns can be used to identify active pathways. EMP, Embden-Meyerhof-Parnas; ED, Entner-Doudoroff; PP, pentose phosphate.

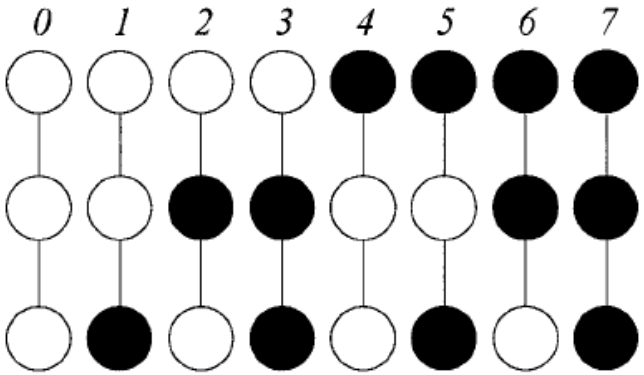

FIG. 1. The eight different positional isotopomers of a C_3 mole
The isotopomers are enumerated from zero to seven, corresponding t
binary number formed using the white circles (^{12}C) as zeros and the sh
circles (^{13}C) as ones.

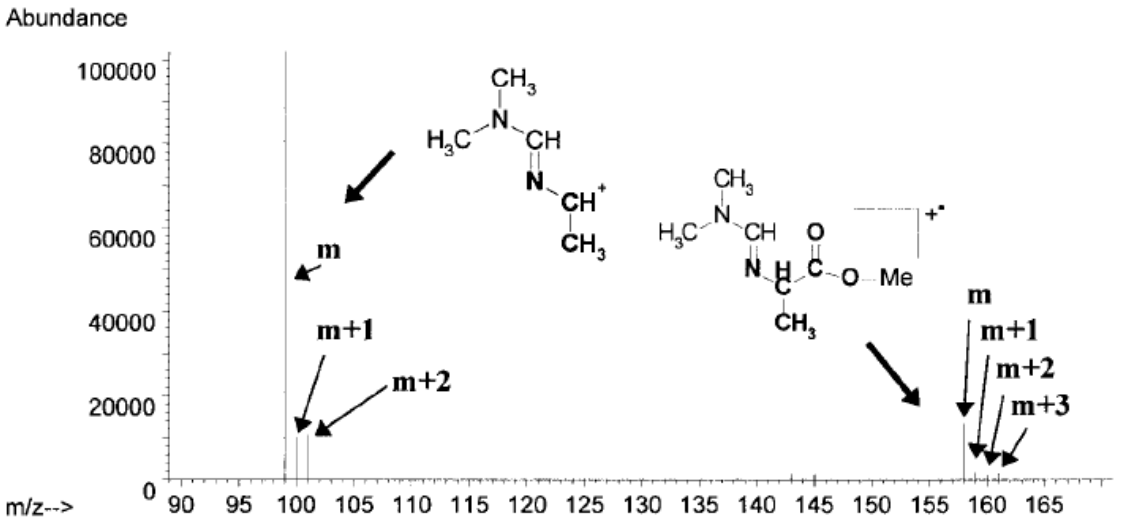

Redes metabólicas em escala genômica.

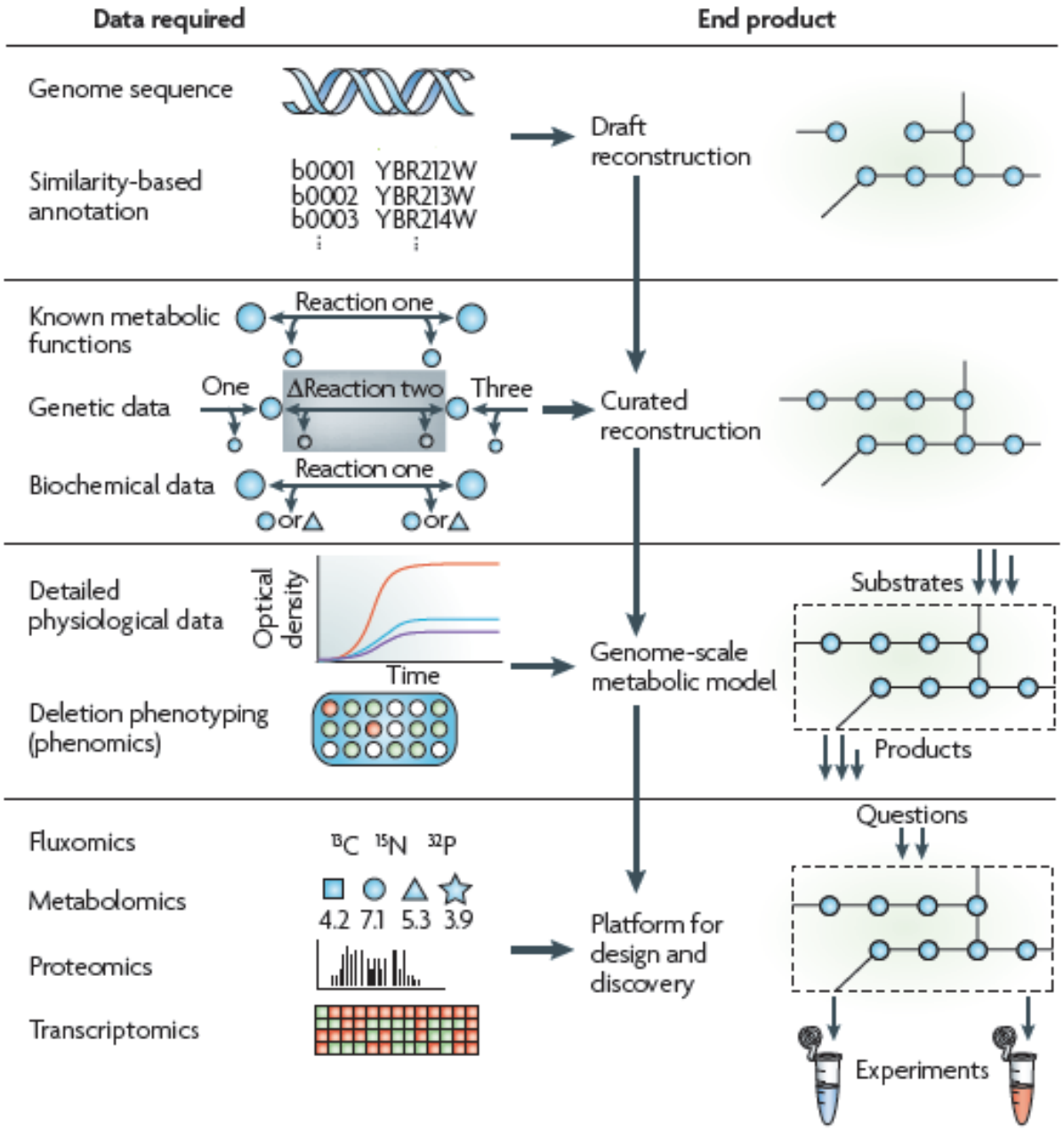

Metabolic Engineering

$$\begin{vmatrix} -1 & 0 & 0 & 0 & 0 & 0 & 0 & 0 & 0 \\ 1 & -1 & 0 & 0 & 0 & 0 & 0 & 0 & 0 \\ 0 & 1 & -1 & 0 & 0 & 0 & 0 & 0 & 0 \\ 0 & 0 & 1 & -1 & 0 & 0 & 0 & 0 & 0 \\ 0 & 0 & 1 & 1 & -1 & 0 & 0 & 0 & 0 \\ 0 & -1 & 0 & 0 & 0 & 1 & 1 & 0 & 0 \\ 0 & 1 & 0 & 0 & 0 & -1 & -1 & 0 & 0 \\ 0 & 0 & 0 & 0 & 1 & -1 & 0 & -1 & 0 \\ 0 & 0 & 0 & 0 & 1 & 0 & 0 & 0 & 0 \\ 0 & 0 & 0 & 0 & 0 & 1 & -1 & 0 & 0 \\ 0 & 0 & 0 & 0 & 0 & 0 & 1 & 0 & 0 \\ 0 & 0 & 0 & 0 & 0 & 0 & 0 & 1 & -1 \\ 0 & 0 & 0 & 0 & 0 & 0 & 0 & 0 & 1 \end{vmatrix} \times \begin{vmatrix} r_1 \\ r_2 \\ r_3 \\ r_4 \\ r_5 \\ r_6 \\ r_7 \\ r_8 \\ r_9 \end{vmatrix}$$

Regulação metabólica

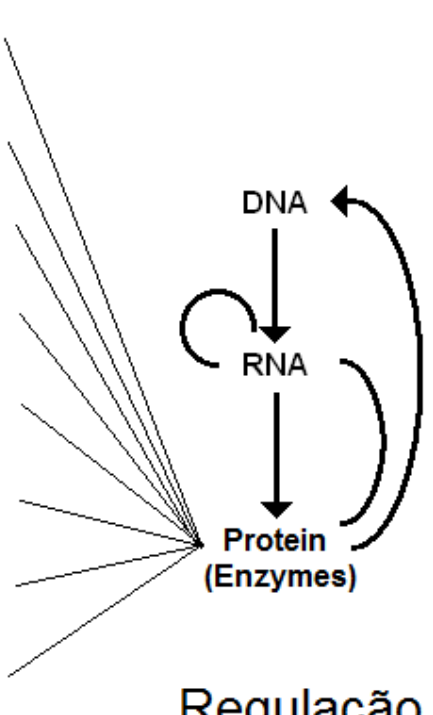

Regulação no nível hierárquico

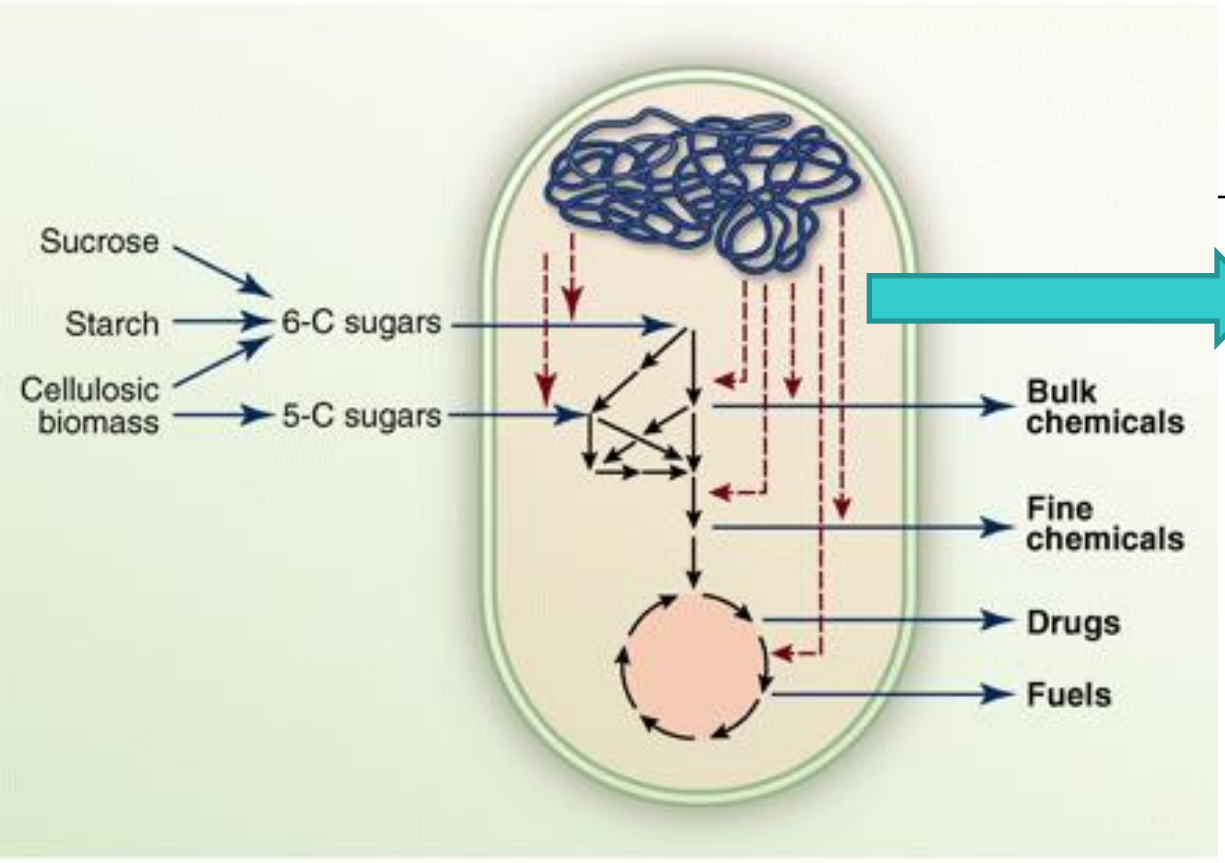
Sucrose
Starch
Cellulosic biomass
6-C sugars
5-C sugars
Bulk chemicals
Fine chemicals
Drugs
Fuels

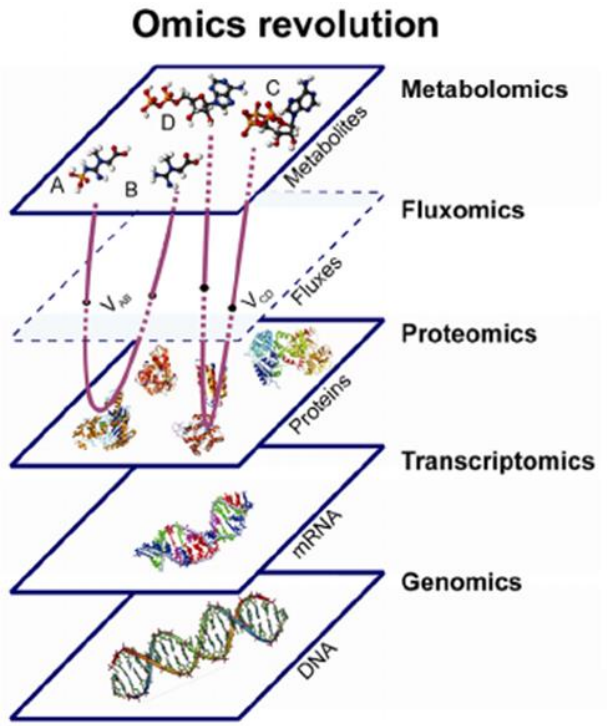
Omics revolution
Metabolomics
Metabolites
A
B
C
D
Fluxomics
Fluxes
Proteomics
Proteins
Transcriptomics
mRNA
Genomics
DNA

Fluxos metabólicos

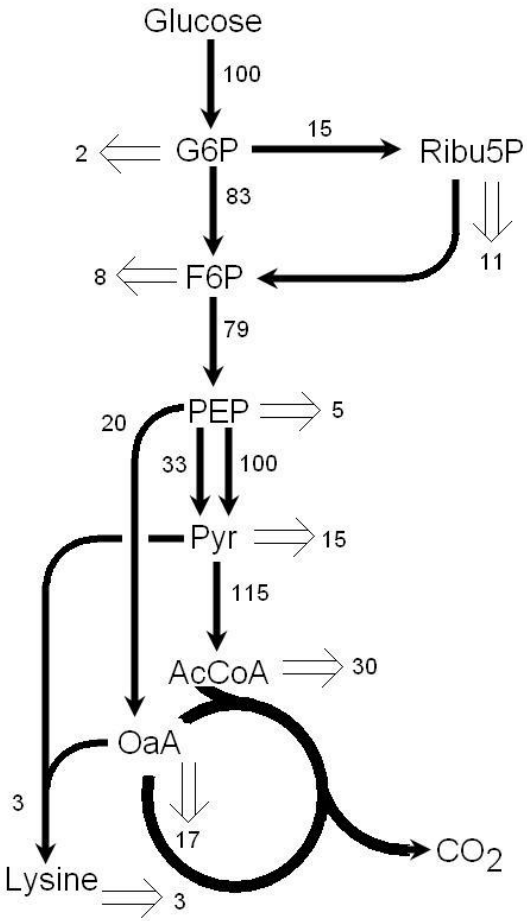

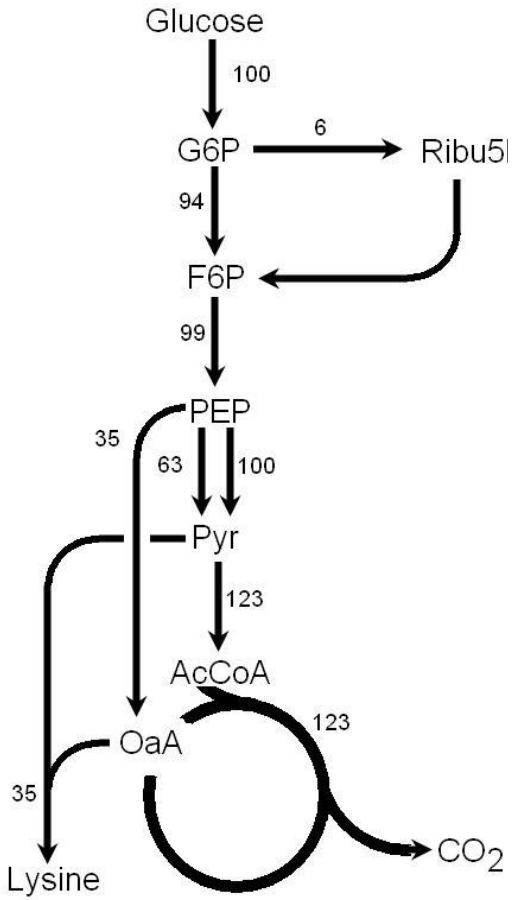

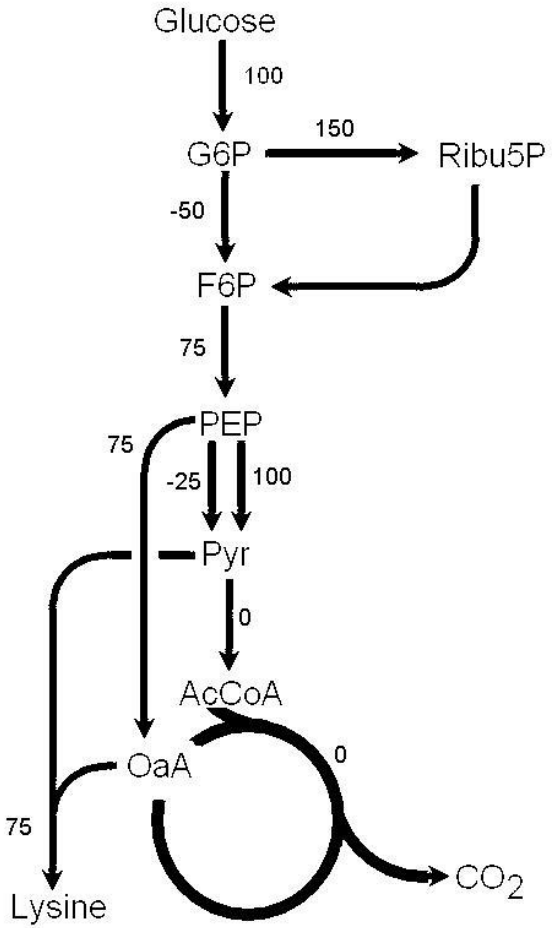

Polyhydroxyalkanoates (PHA)

A family of polyesters accumulated by bacteria.

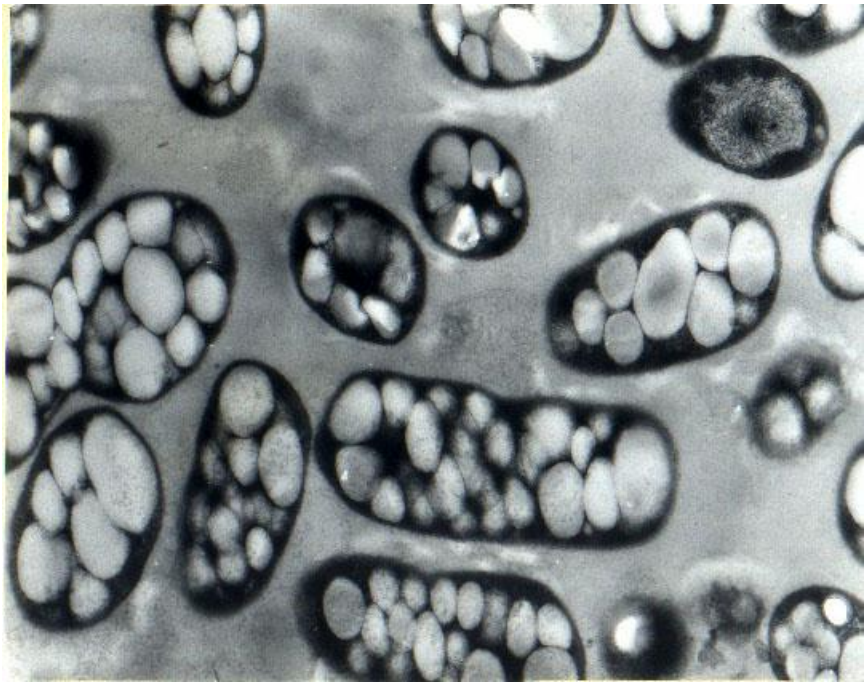

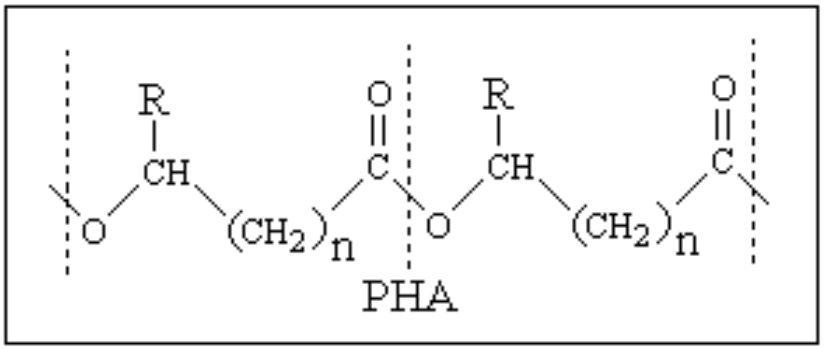

PHA production integrated to a sugar and etanol mill.

IPT
Instituto de Pesquisas Tecnológicas

COPERSUCAR

USP
UNIVERSIDADE DE SÃO PAULO

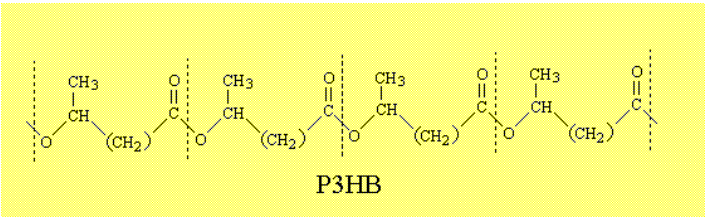

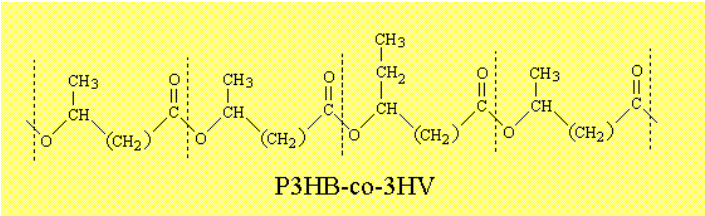

R. V. Nonato · P. E. Mantelatto · C. E. V. Rossell

Integrated production of biodegradable plastic, sugar and ethanol

Appl Microbiol Biotechnol (2001) 57:1–5
DOI 10.1007/s002530100732

MINI-REVIEW

A green cycle for simultaneous poly 3-hydroxybutyric acid, sugar and ethanol production

Polihidroxialcanoatos (PHA) Termoplásticos

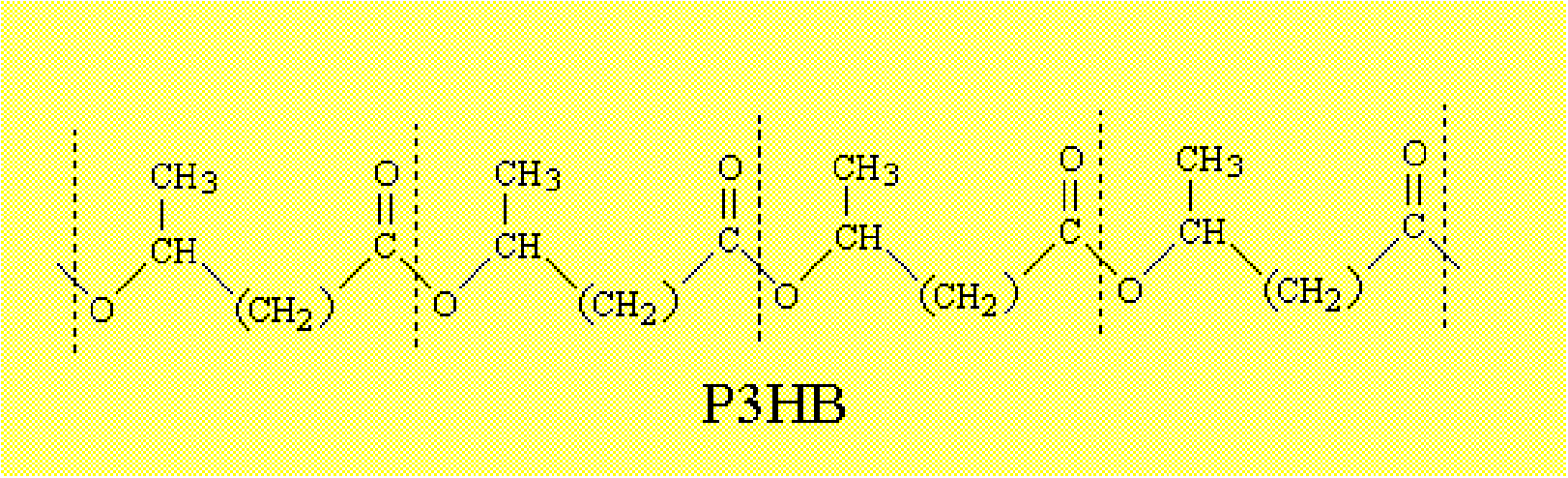

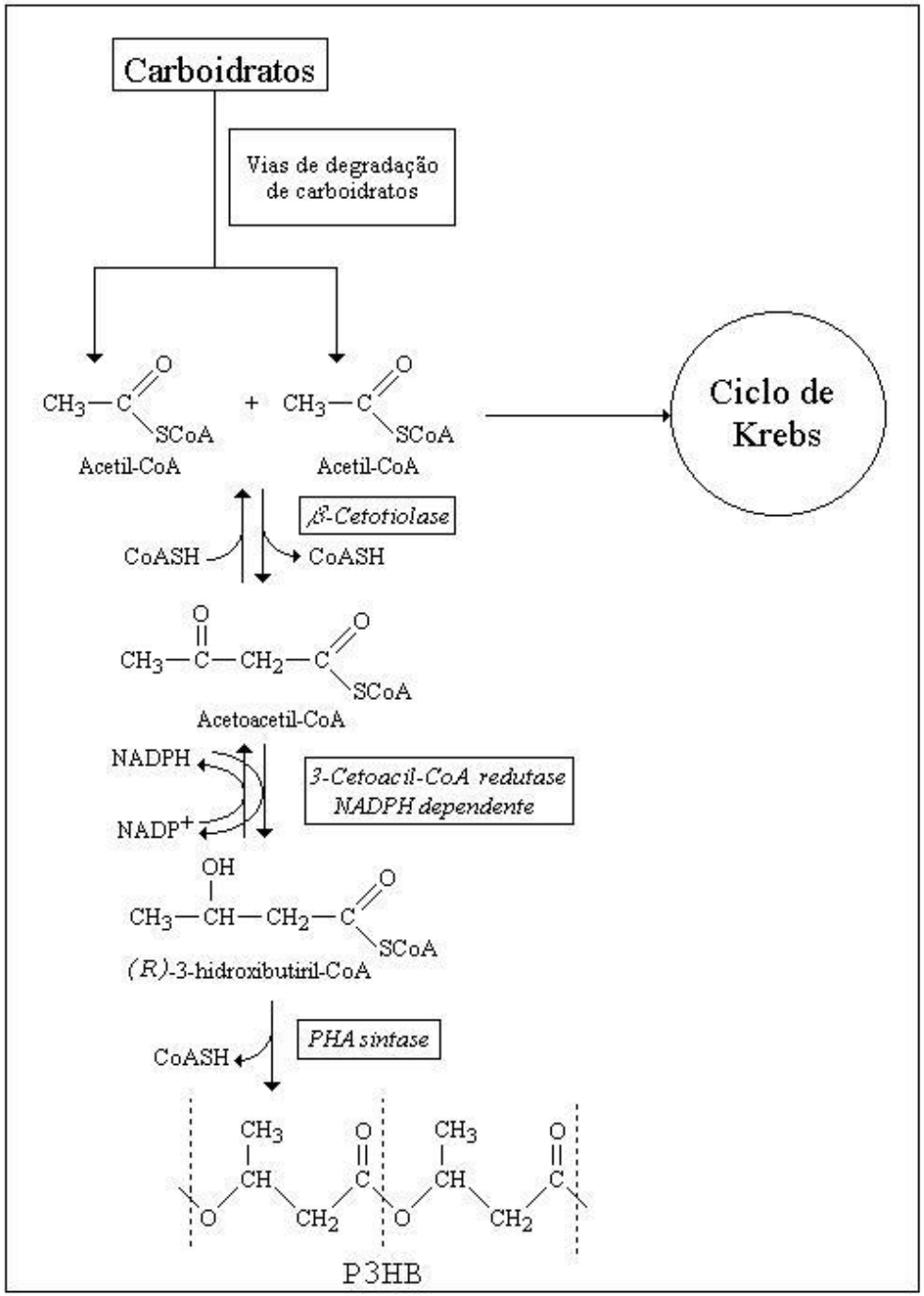
Carboidratos
Vias de degradação de carboidratos
Acetil-CoA
Acetil-CoA
Ciclo de Krebs
β-Cetotiolase
CoASH
CoASH
Acetoacetil-CoA
NADPH
NADP+
3-Cetoacil-CoA redutase NADPH dependente
(R)-3-hidroxibutiril-CoA
CoASH
PHA sintase
P3HB

P3HB - Produção

Linhagens	Carboidrato	Carboidratos residuais			MSC	P3HB	
		S	G	F	(g/L)	%MSC	$Y_{P/S}$
R.eutropha	G+F	-	1,9	0,0	6,56	76,7	0,35
IPT 086	G+F	-	89,3	0,0	4,32	62,5	0,32
	S	107,4	0,0	0,0	0,35	1,5	0,00
IPT 083	G+F	-	0,0	0,0	6,78	68,5	0,30
	S	0,0	0,0	0,0	6,37	60,9	0,27
IPT 101	G+F	-	0,0	0,0	5,59	74,6	0,29
	S	0,0	0,0	0,0	6,14	68,4	0,29
IPT 076	G+F	-	0,0	0,0	6,31	63,6	0,25
	S	0,0	0,0	0,0	6,46	56,2	0,26

P3HB production from sugarcane carbohydrates

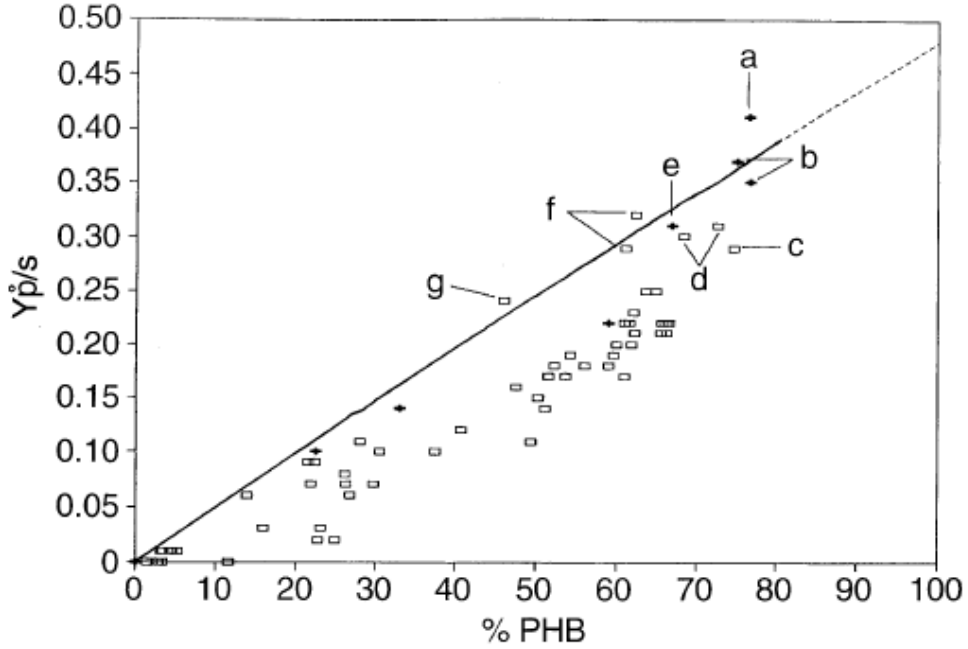

$$Y^{O}_{P/C} = \frac{PHB}{PHB\left(\frac{1}{Y^{T}_{P/C}} - \frac{1}{Y_{X/C}}\right) + \frac{100}{Y_{X/C}}}$$

Fig. 1 Relation between $Y^{O}_{P/C}$ and poly-(3-hydroxybutyrate) (*PHB*) content for different strains isolated from soil (□) or obtained from the culture collection (+) when glucose plus fructose was used as the carbon source. The line represents the values expected when $Y^{T}_{P/C} = 0.48$ g/g and $Y_{X/C} = 0.50$ g/g. Points related to strains *A. latus* DSM 1123 (*a*), *A. eutrophus* DSM 545 (*b*), IPT-101 (*c*), IPT-083 (*d*), *A. eutrophus* DSM 428 (*e*), IPT-086 (*f*), and IPT-055 (*g*) are indicated

Análise de fluxos - Balanços metabólicos

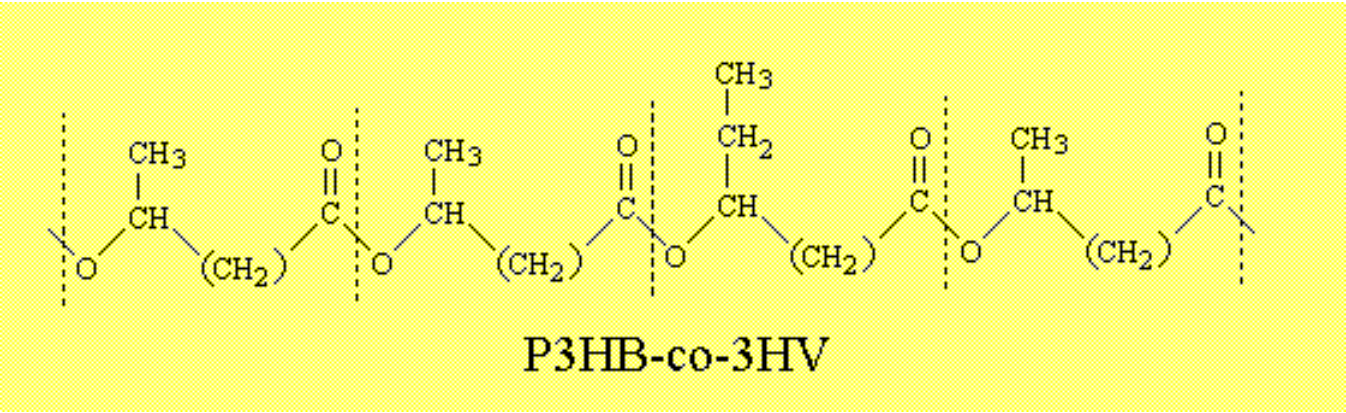

Análise de fluxos - Balanços metabólicos

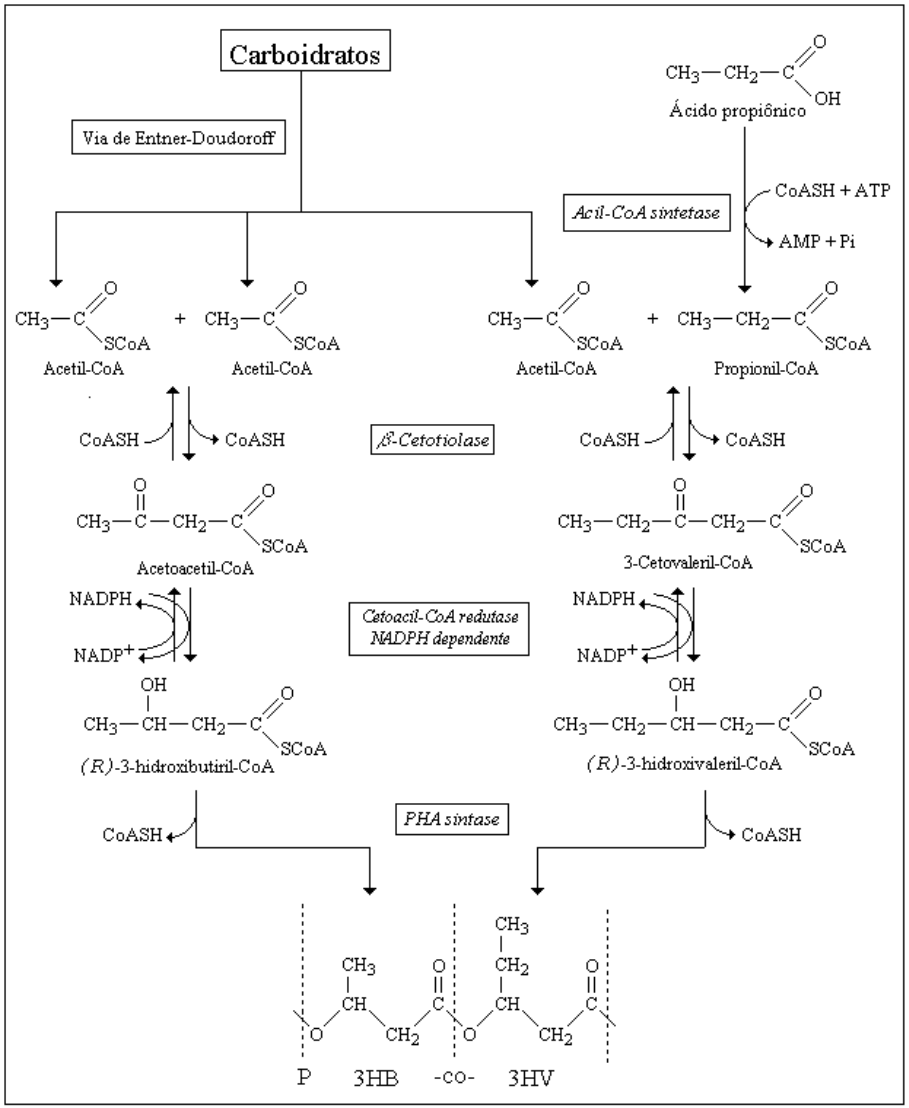

P3HB-*co*-3HV production from carbohydrates and propionic acid

Strains	CDW (g/l)	Residual carbohydrates (%)	PHA			
			CDW %	3HB (mol%)	3HV (mol%)	$Y_{3HV/PROP}$ (g/g)
A. eutrophus DSM 545	3.92	0.0	71.4	96.1	3.9	0.13
A. latus DSM 1123	0.95	101.8	14.6	55.0	45.0	0.07
P. cepacia DSM 50181	3.35	1.9	38.4	97.3	2.7	0.04
IPT-040	3.77	1.7	32.3	97.1	2.9	0.05
IPT-044	3.92	1.7	51.1	97.1	2.9	0.07
IPT-045	3.73	0.0	49.4	96.2	3.8	0.08
IPT-048	2.97	0.0	44.3	96.2	3.8	0.06
IPT-055	4.27	72.2	1.5	100.0	0.0	0.00
IPT-056	3.60	31.3	30.9	98.5	1.5	0.02
IPT-076	5.06	1.9	56.8	97.1	2.9	0.10
IPT-083	4.89	5.2	56.8	96.9	3.1	0.10
IPT-086[a]	2.06	75.4	39.0	89.9	10.1	0.09
IPT-098	5.90	0.0	17.7	94.7	5.3	0.07
IPT-101	2.98	41.8	32.3	95.4	4.6	0.05

[a] Fructose instead of glucose was supplied

Maximum theoretical yield = 1.35 g/g

P3HB-*co*-3HV production from carbohydrates and propionic acid

Efficiency of *B. sacchari* mutants in converting propionic acid to 3HV units.

Strain	Phenotype	Results		
		3HB mol%	3HV mol%	$Y_{3HV/prp}$ (g/g)[c]
IPT 101[d]	wild type	93.8	6.2	0.10
IPT 183	I	84.1	15.9	0.34
IPT 185	II	82.6	17.4	0.35
IPT 190	III	80.1	19.9	0.37
IPT-195	IV	39.0	61.0	0.81
IPT 196	IV	33.2	66.8	0.78
IPT 189	IV	44.7	55.3	0.81
IPT 189	feeding strategies of suc/prp			1.34

Silva *et al.*, 2000

Rocha *et al.*, 2008

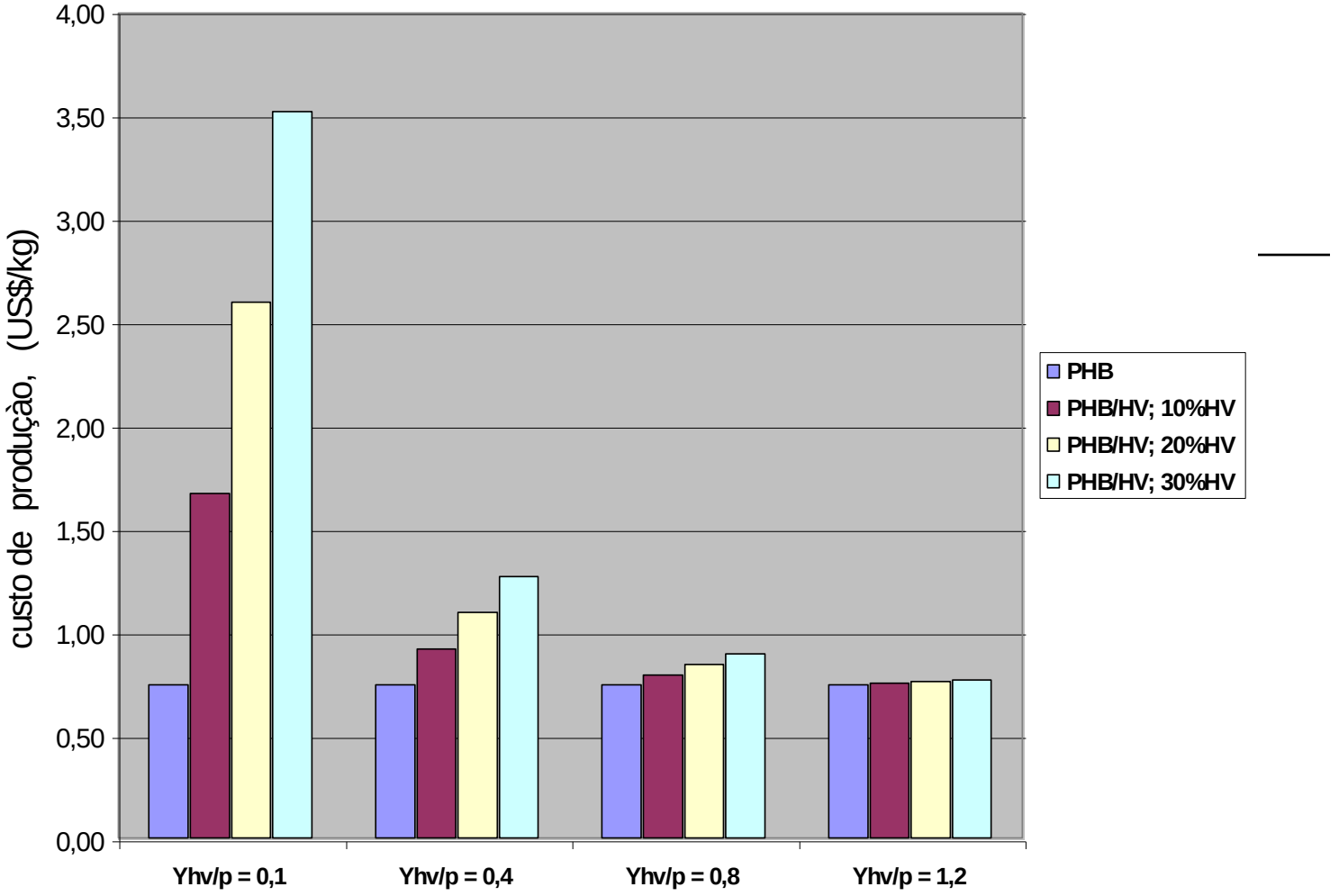

Carbon source cost

Alta densidade celular

Requirida para aumentar produtividades volumétricas.

Em processo em batelada alimentada.

Em processo contínuo.

Alta densidade celular

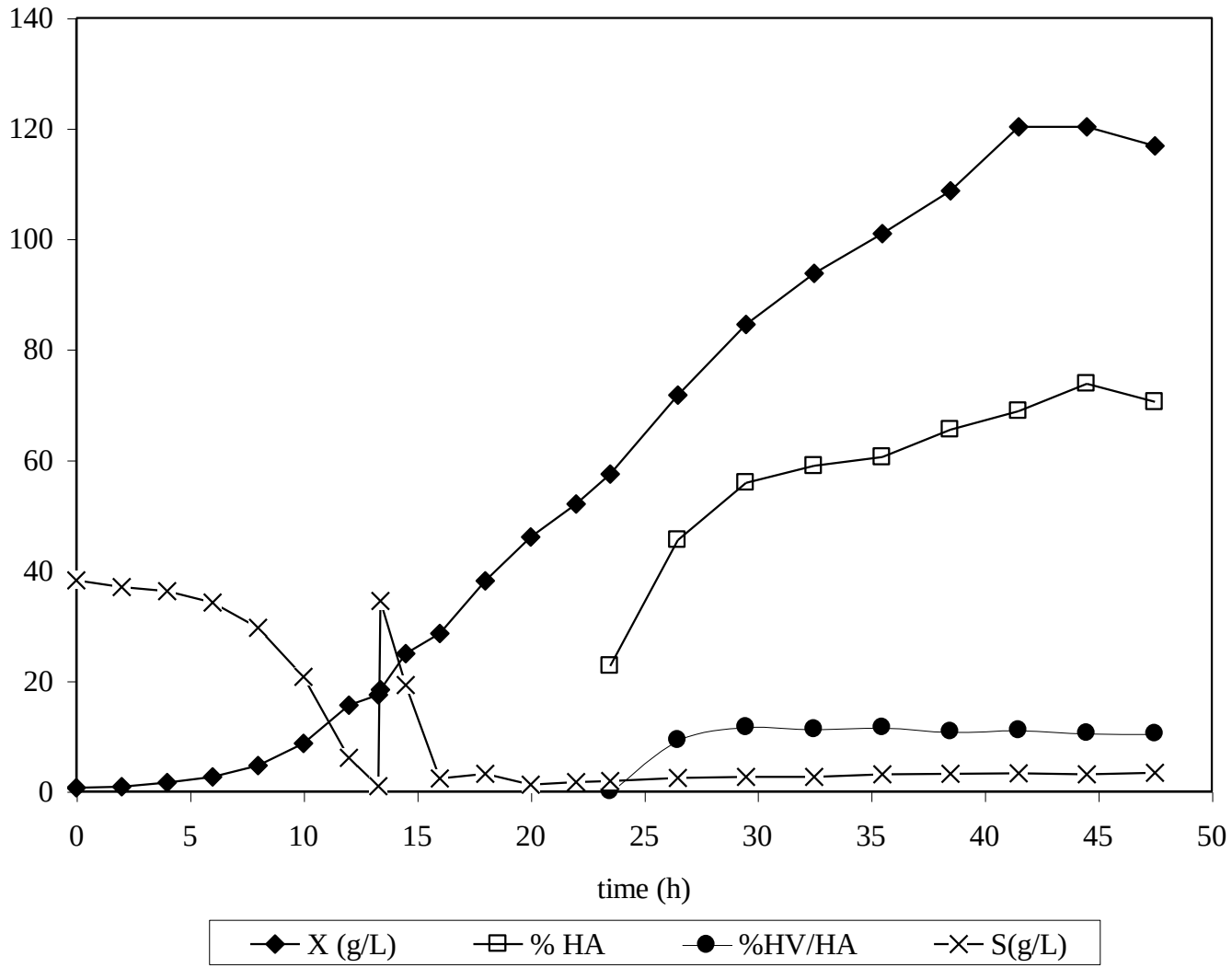

Integrated PHB, Sugar and Ethanol Mill

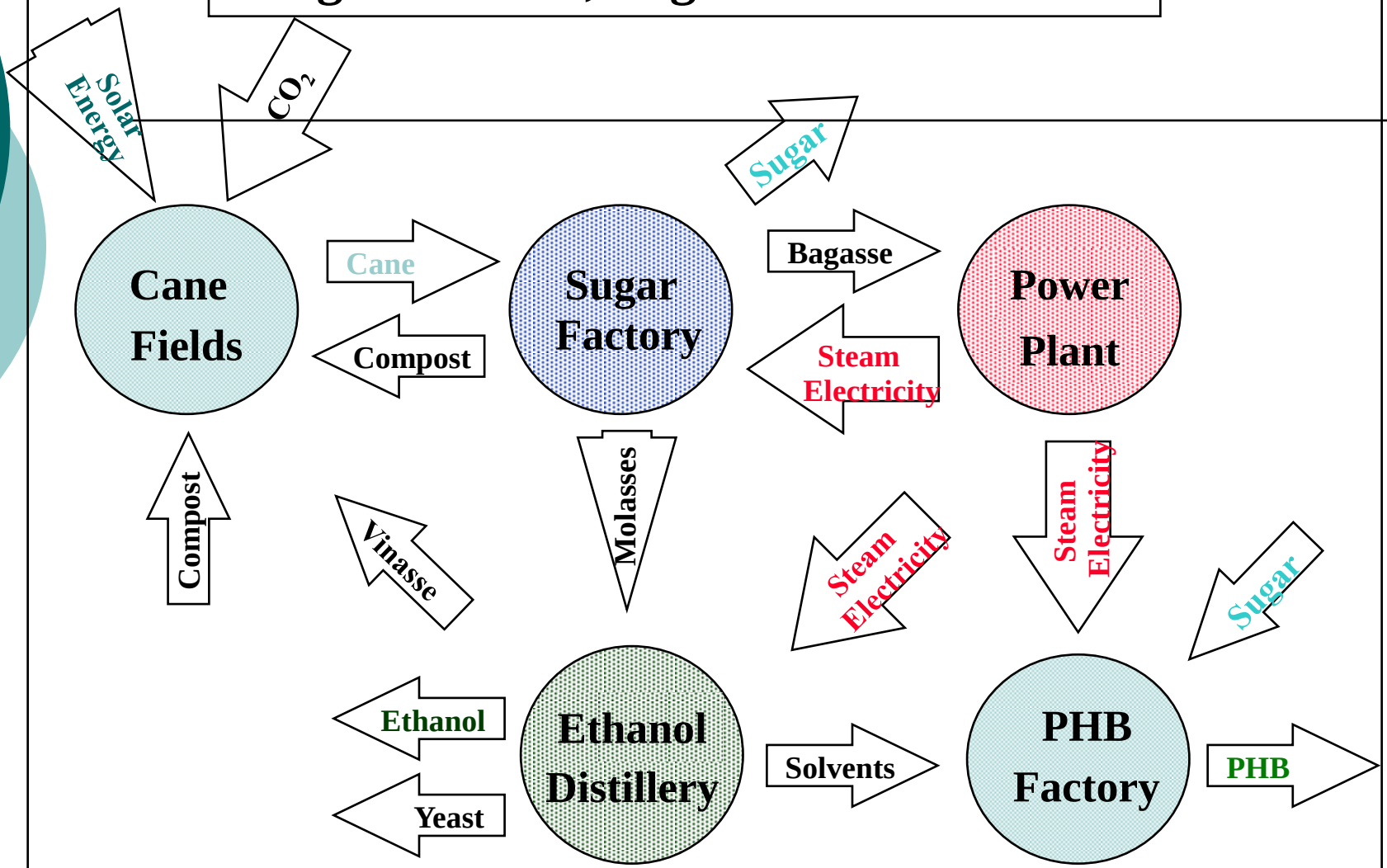

Produtos de Base biológica

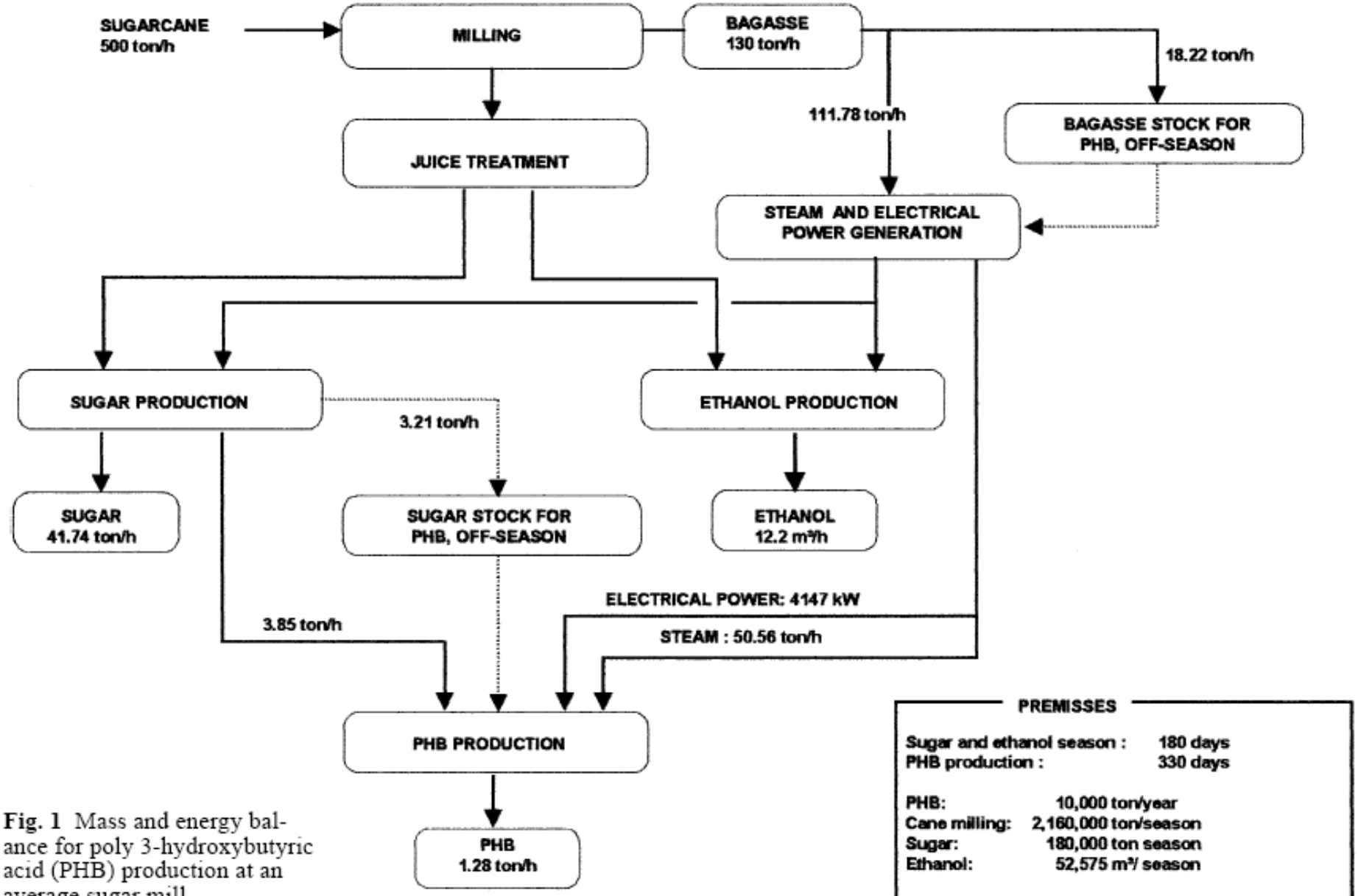

Fig. 1 Mass and energy balance for poly 3-hydroxybutyric acid (PHB) production at an average sugar mill

PHA are biobased polymers for biorefineries.

R. V. Nonato · P. E. Mantelatto · C. E. V. Rossell

Integrated production of biodegradable plastic, sugar and ethanol

A green cycle for simultaneous poly 3-hydroxybutyric acid, sugar and ethanol production

Appl Microbiol Biotechnol (2001) 57:1–5
DOI 10.1007/s002530100732

MINI-REVIEW

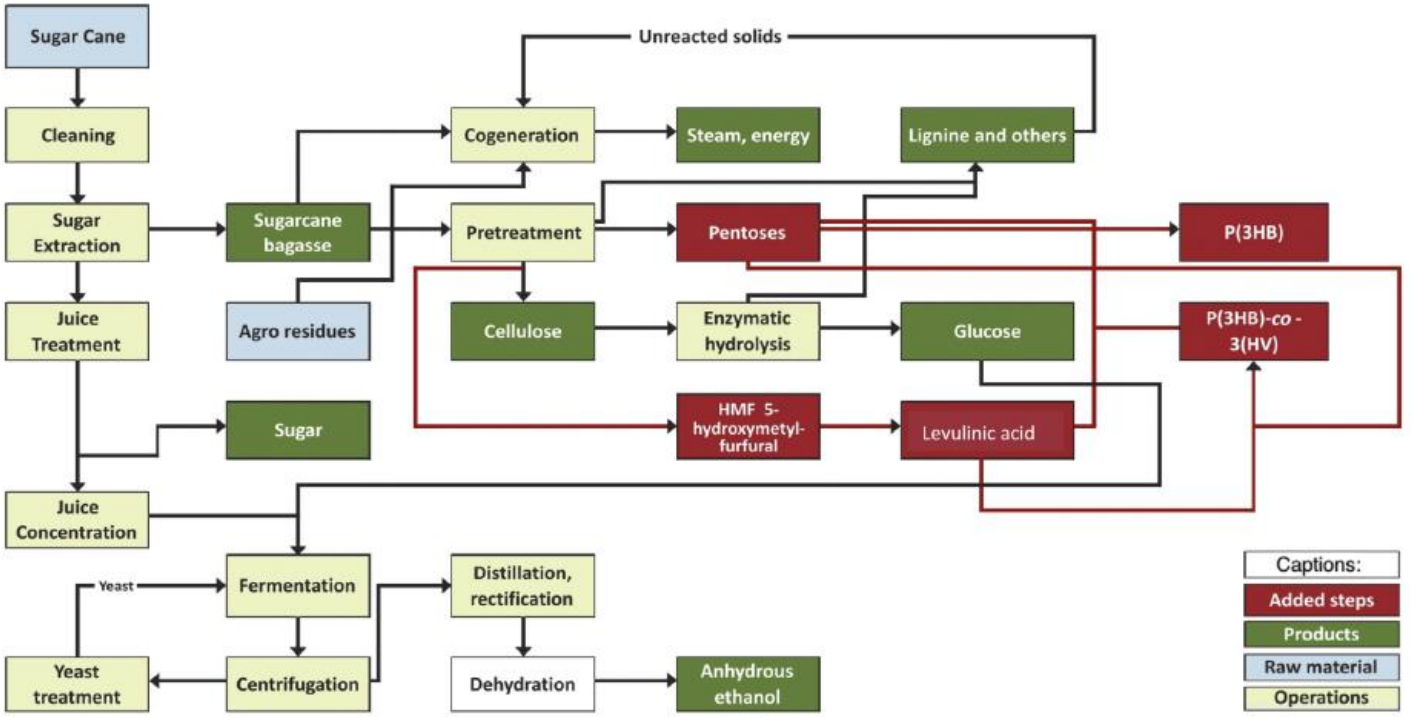

Fig. 1. Steps integrating ethanol and biopolymer production from sugarcane in the context of a biorefinery (modified from Kam & Kam, 2006 [84] by Raicher [82]). Sugar is extracted from the sugarcane, leaving the concentrated juice and bagasse. The concentrated juice is subjected to yeast fermentation to ethanol. Yeast is recycled to a new fermentation. The bagasse and other agricultural residues, such as sugarcane leaves, can have two destinations: cogeneration of steam and energy for the plant, or pretreatment to release cellulose, pentoses and hydroxy methylfurfural (HMF). Cellulose can be hydrolyzed enzymatically, releasing glucose that can be used in the production of ethanol 2G. From HMF, levulinic acid can be produced and used, associated to the pentoses, in the production of PHA.

PHA production integrated to a sugar and etanol mill.

IPT
Instituto de Pesquisas Tecnológicas

COPERSUCAR

USP
UNIVERSIDADE DE SÃO PAULO

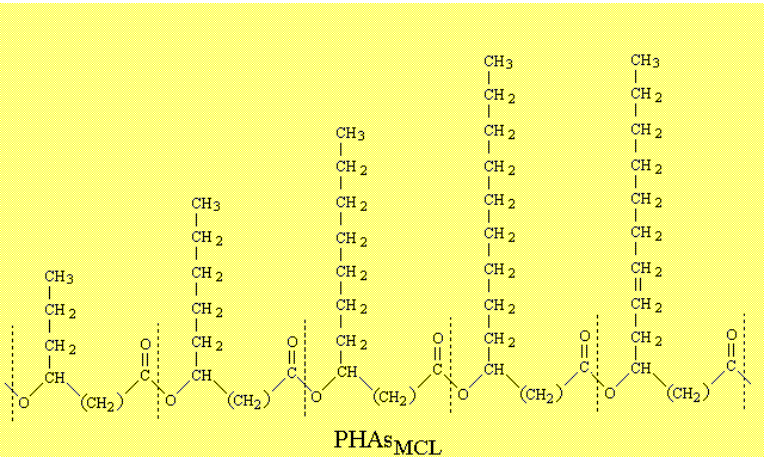

R. V. Nonato · P. E. Mantelatto · C. E. V. Rossell

Integrated production of biodegradable plastic, sugar and ethanol

Appl Microbiol Biotechnol (2001) 57:1–5
DOI 10.1007/s002530100732

MINI-REVIEW

A green cycle for simultaneous poly 3-hydroxybutyric acid, sugar and ethanol production

$$Y^{G}_{PHA/G} = \frac{\%PHA}{\frac{100}{Y_{Xr/G}} - \frac{\%PHA}{Y_{Xr/G}} + \frac{\%3HHx}{Y_{3HHx/G}} + \frac{\%3HO}{Y_{3HO/G}} + \frac{\%3HD}{Y_{3HD/G}} + \frac{\%3HDd}{Y_{3HDd/G}}}$$

Table 1. Production of PHA_{MCL} from carbohydrates by some sugarcane soil isolates.

Bacterial strain	CDW (g/L)	PHA composition (mol%)				PHA (%CDW)	$Y^{G}_{PHA/G}$ (g/g)	$\%Y_{MAX}$
		3HHx	3HO	3HD	3HDd			
KT2440	3.96	3.25	12.48	79.88	4.39	48.52	0.127	60.0
LFM046	3.72	5.01	21.85	71.83	1.31	60.51	0.161	62.9
LFM047	2.21	1.72	22.88	61.81	13.58	13.99	0.023	34.3
LFM050	2.50	0.92	15.98	67.75	15.35	18.55	0.037	41.9
LFM065	4.06	0.00	8.88	87.81	3.30	30.52	0.084	60.6

CDW – Cell dry weight 3HHx - 3-hydroxyhexanoic acid 3HO - 3-hydroxyoctanoic acid
3HD - 3-hydroxydecanoic acid 3HDd - 3-hydroxydodecanoic acid $Y^{G}_{PHA/G}$ – global PHA yield from glucose
$\%Y_{MAX}$ - percentual of the maximum theoretical yield.

Cultivo contínuo

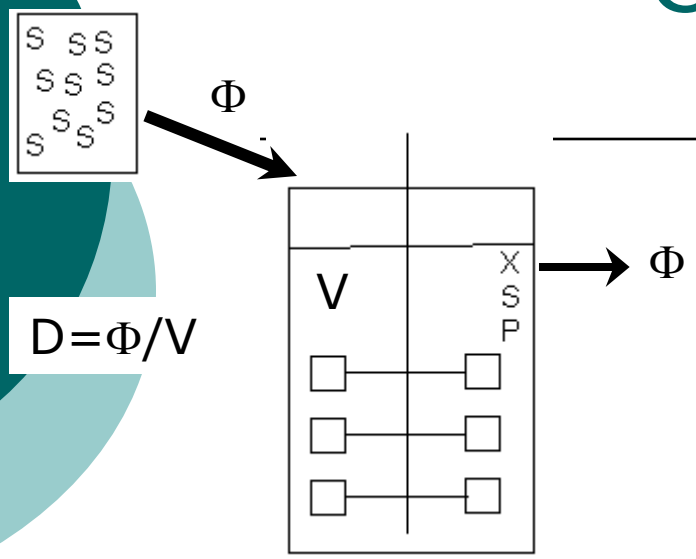

$$V\frac{dX}{dt} = \Phi X_o - \Phi X + V\left(\frac{dX}{dt}\right)_{crescimento}$$

Sendo que

$$\left(\frac{dX}{dt}\right)_{crescimento} = \mu X \qquad D = \frac{\Phi}{V}$$

Temos

$$\frac{dX}{dt} = D\,(X_o - X) + \mu X$$

Como Xo = 0 (meio estéril)

$$\frac{dX}{dt} = \mu X - DX$$

No estado estacionário dX/dt = 0

$$\mu X = DX$$

OU

$$\mu = D$$

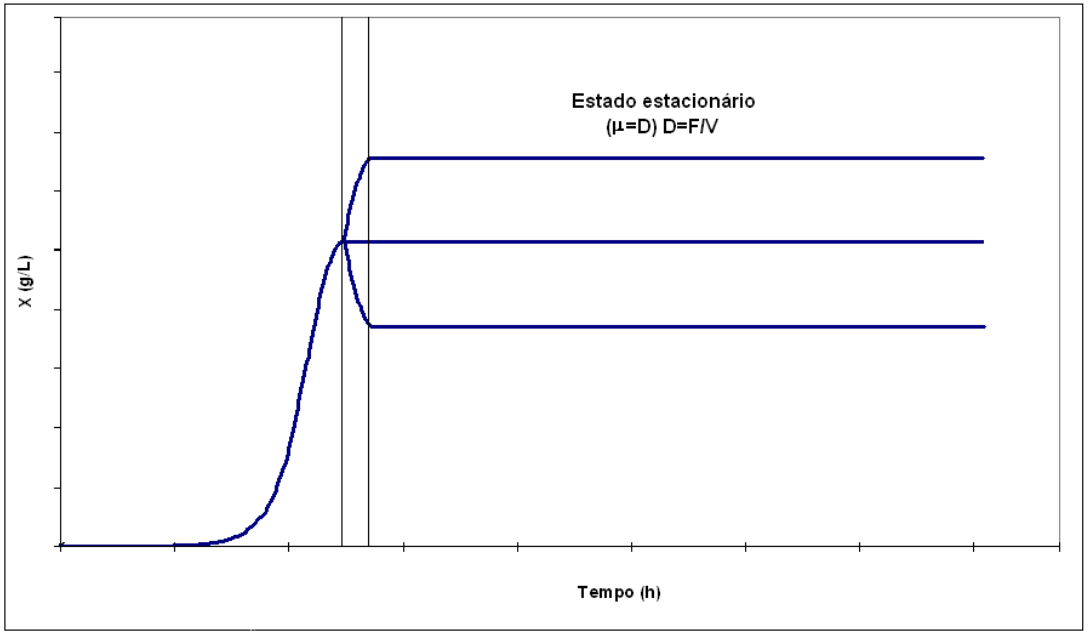

Metabolic fluxes analysis

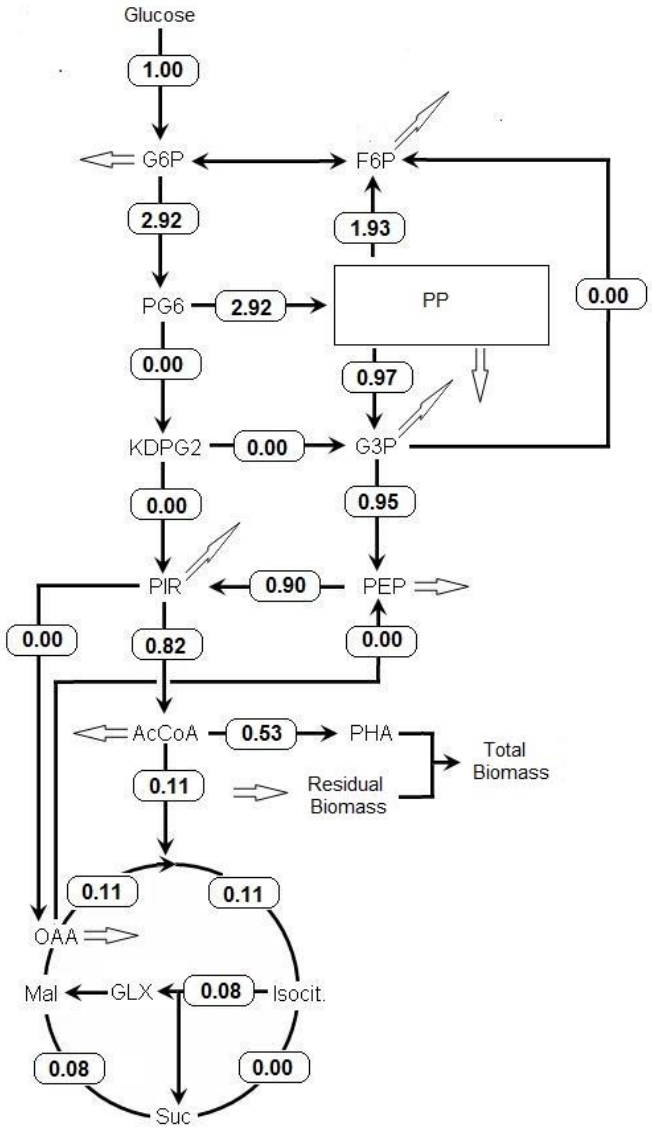

Fluxes distribution for PHA production by *Pseudomonas* sp. from glucose.

Elementary Mode analysis

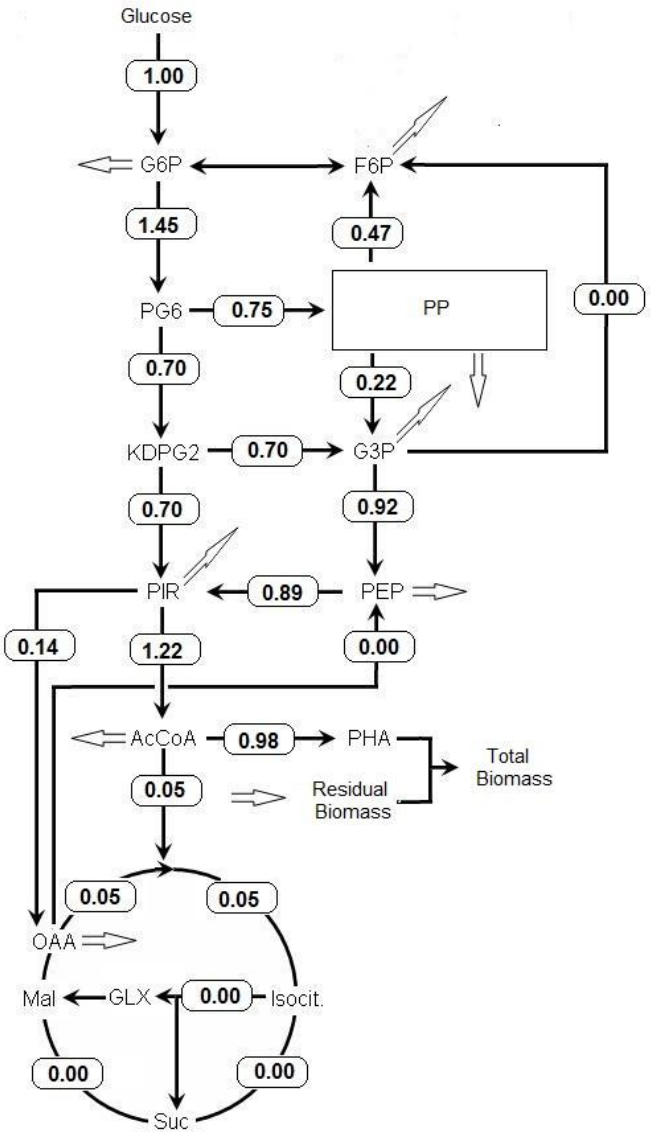

Optimal fluxes distribution for PHA production by *Pseudomonas* sp. from glucose.

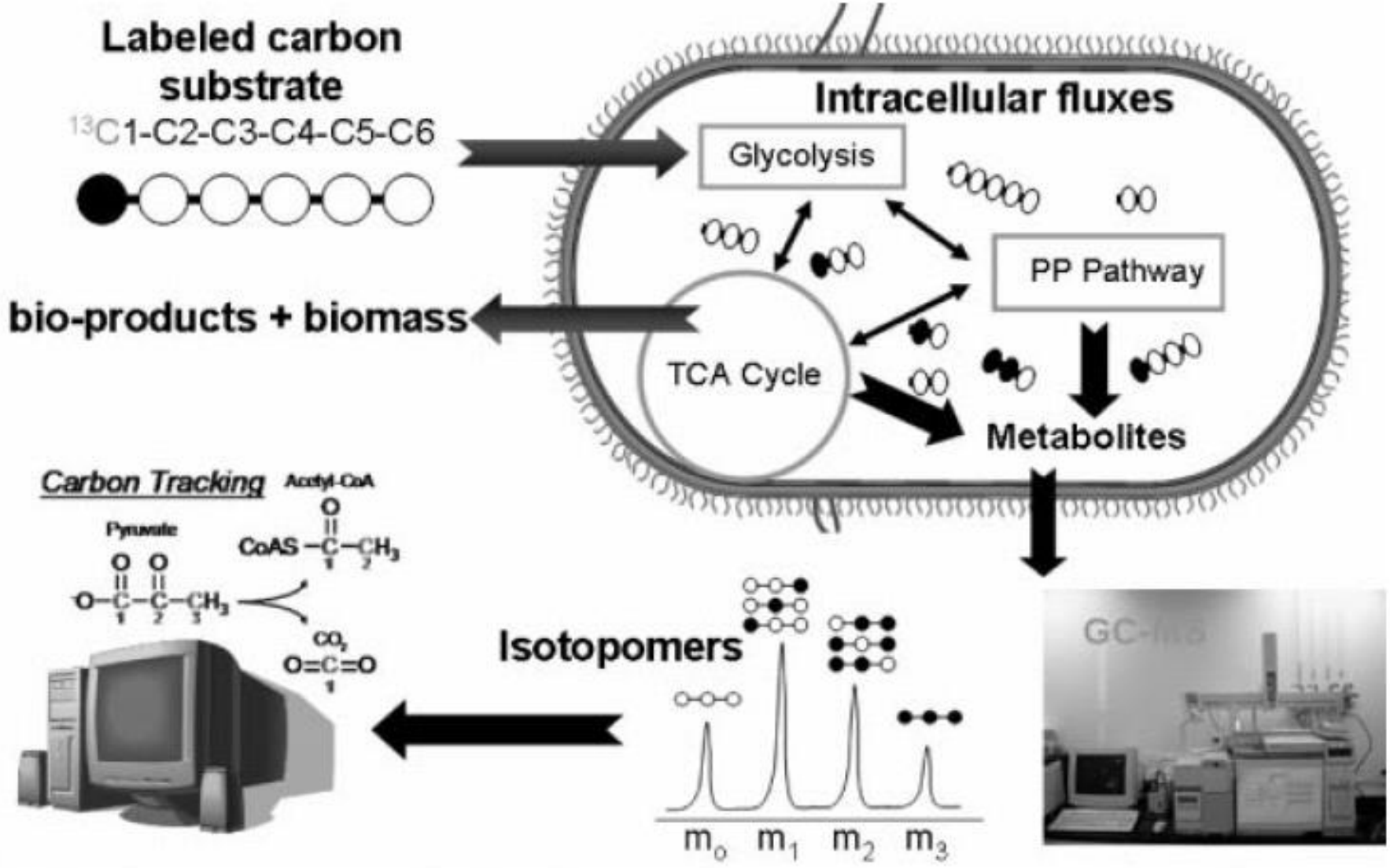

FIGURE 2. Protocol for ^{13}C-based flux analysis. [Color figure can be viewed in the online issue, which is available at www.interscience.wiley.com.]

Mass Spectrometry Reviews, **2009**, *28*, 362–375

Análise de fluxos – Experimentos com traçadores

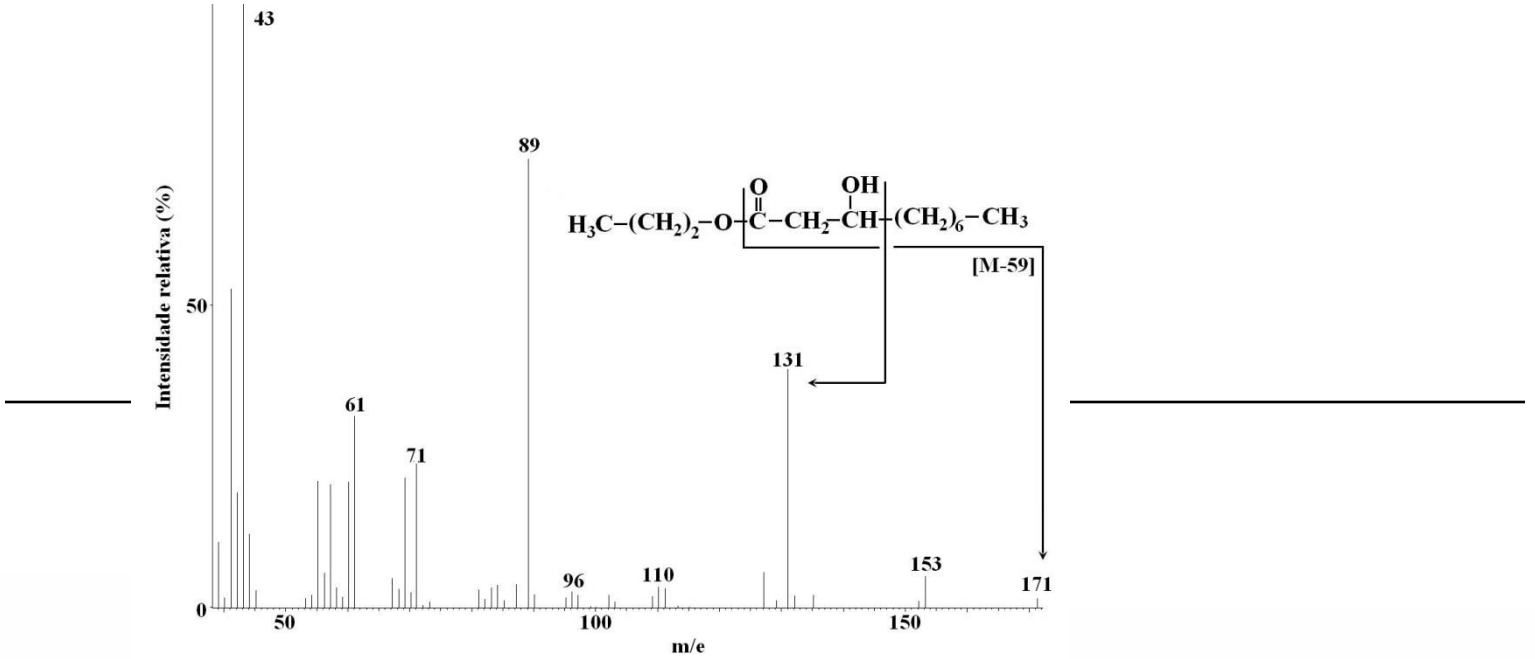

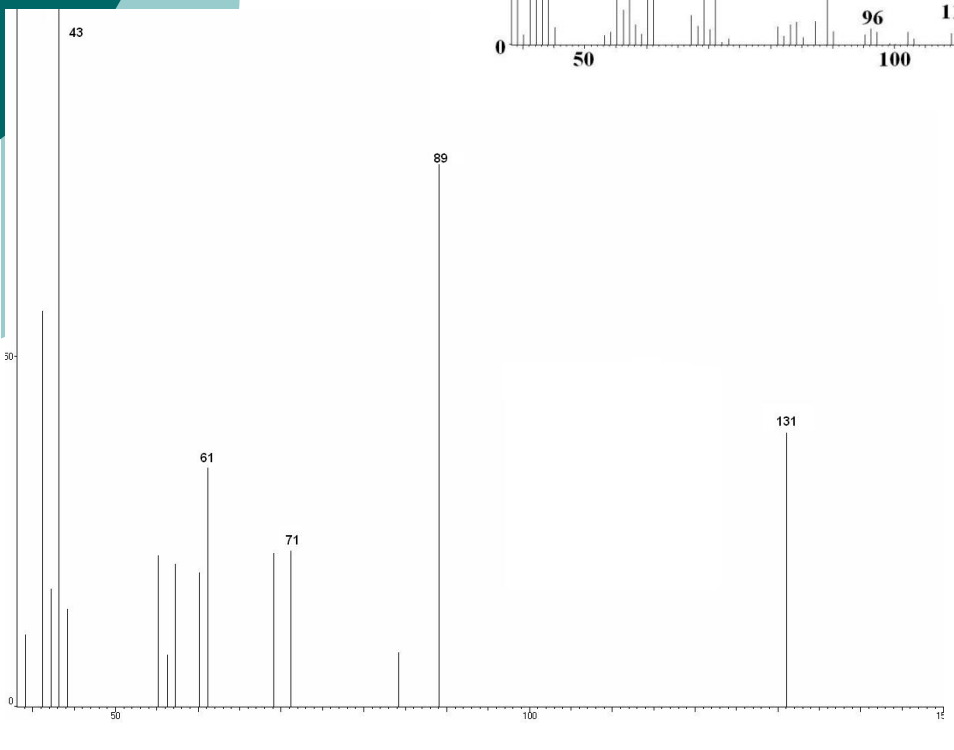

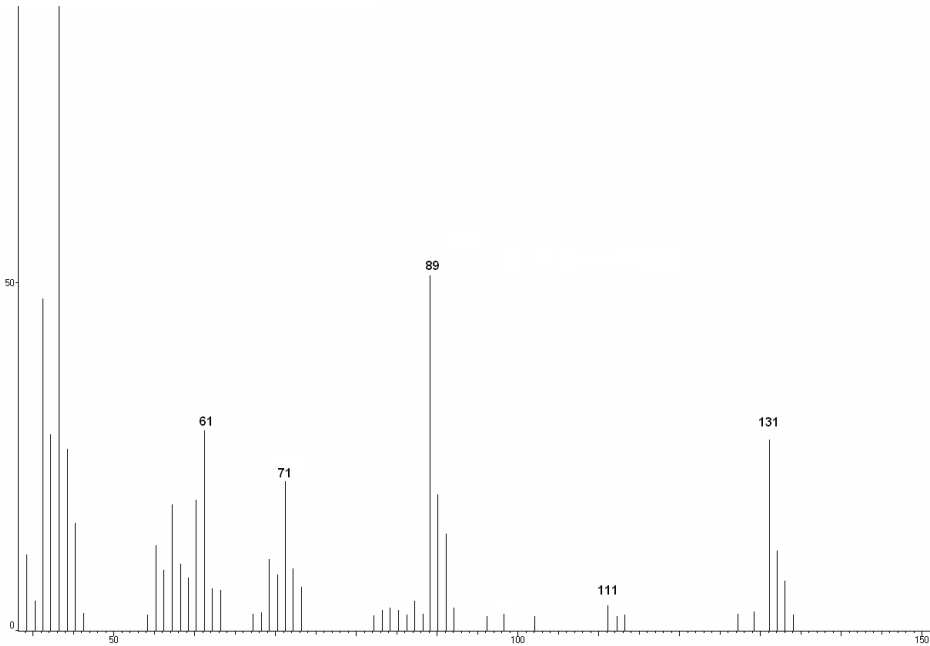

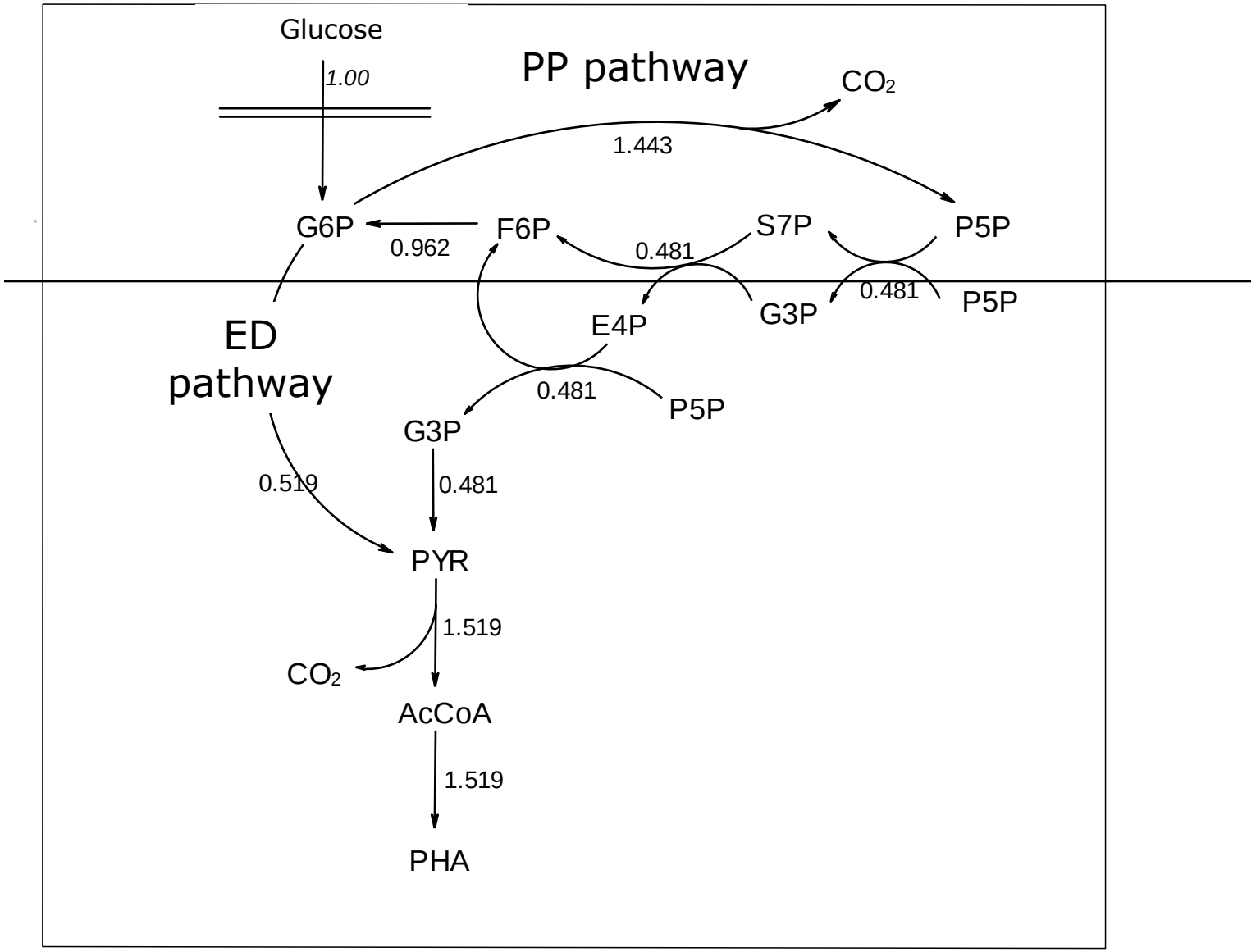
Glucose
1.00
PP pathway
CO2
1.443
G6P
0.962
F6P
S7P
0.481
P5P
0.481
G3P
P5P
E4P
ED
pathway
0.481
P5P
G3P
0.519
0.481
PYR
1.519
CO2
AcCoA
1.519
PHA

Genomic scale metabolic networks

genomeA
Journals.ASM.org

Draft Genome Sequence of *Pseudomonas* sp. Strain LFM046, a Producer of Medium-Chain-Length Polyhydroxyalkanoate

Juliana Cardinali-Rezende,[a] Paulo Moises Raduan Alexandrino,[a,b] Rafael Augusto Theodoro Pereira de Souza Nahat,[a] Débora Parrine Vieira Sant'Ana,[a*] Luiziana Ferreira Silva,[a] José Gregório Cabrera Gomez,[a] Marilda Keico Taciro[a]

Institute of Biomedical Sciences, University of São Paulo, São Paulo, Brazil[a]; Department of Computer Science, Institute of Mathematics and Statistics, University of São Paulo, São Paulo, Brazil[b]

* Present address: Débora Parrine Vieira Sant'Ana, Department of Bioresource Engineering, McGill University, Montreal, Quebec, Canada.

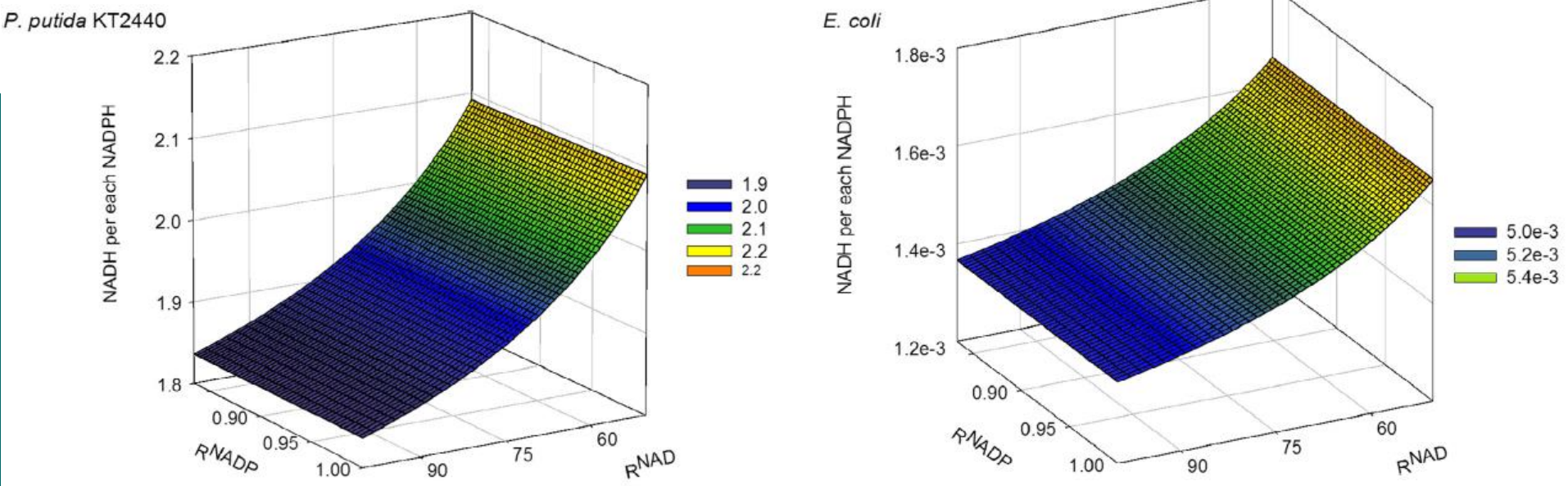

Fig. 4. Relative productions of NADH respect to NADPH during the oxidation of G6P catalyzed by the enzymes PputG6PDH-1 (top) and EcG6PDH (bottom), depending on the concentrations ratios (R) of the oxidized and reduced forms of NAD(H) and NADP(H). The represented values were obtained assuming a concentration of G6P of 1 mM.

Table 3
GND specific activities, using NAD or NADP as cofactors, registered in crude cellular extracts from *E. coli* MG1655 and *P. putida* KT2440 grown in mineral medium with glucose as the sole carbon source.

Bacteria	[a]Activity with NAD (nmol mg_{prot}^{-1} min^{-1})	[a]Activity with NADP (nmol mg_{prot}^{-1} min^{-1})
E. coli MG1655	8 ± 1.5	103 ± 0.4
P. putida KT2440	25 ± 0.4	6 ± 0.4

FEBS Open Bio 2 (2012) 308–315
Journal homepage: www.elsevier.com/locate/feprobeupio

Quantifying NAD(P)H production in the upper Entner–Doudoroff pathway from *Pseudomonas putida* KT2440

Karel Olavarria *, Marina Pupke Marone, Henrique da Costa Oliveira, Juan Camilo Roncallo, Fernanda Nogales da Costa Vasconcelos, Luiziana Ferreira da Silva, José Gregório Cabrera Gomez

Departmento de Microbiologia, Instituto de Ciências Biomédicas, Universidade de São Paulo, Brazil

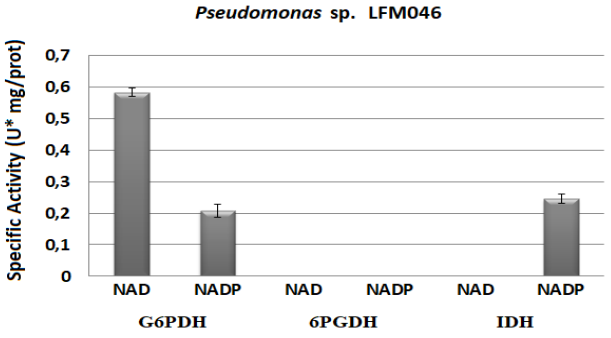

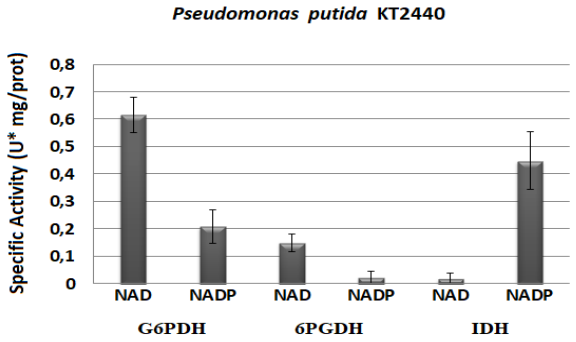

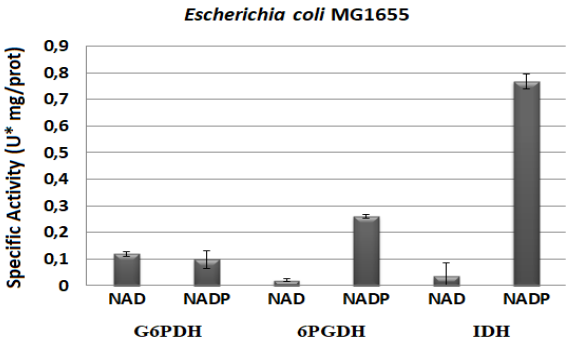

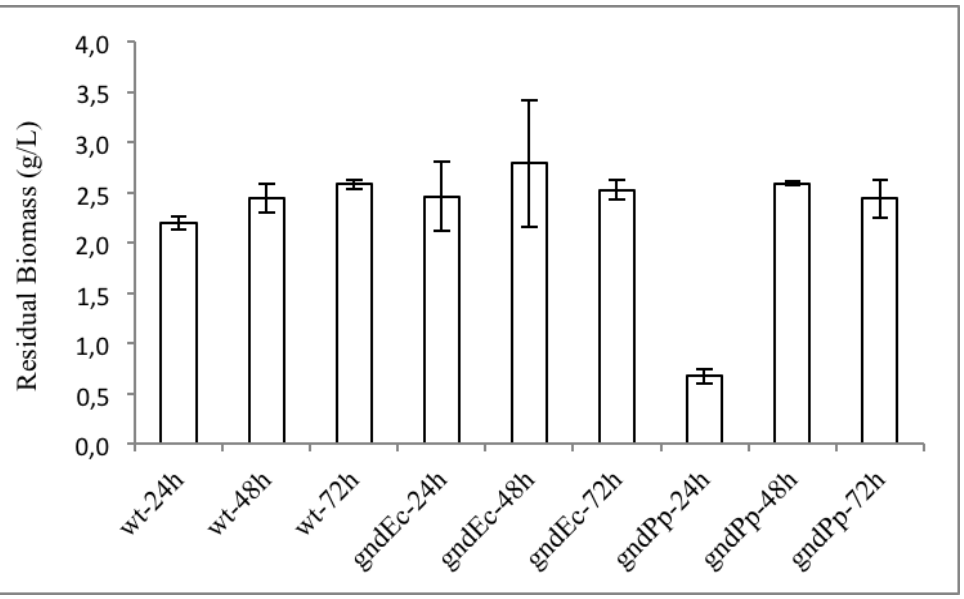

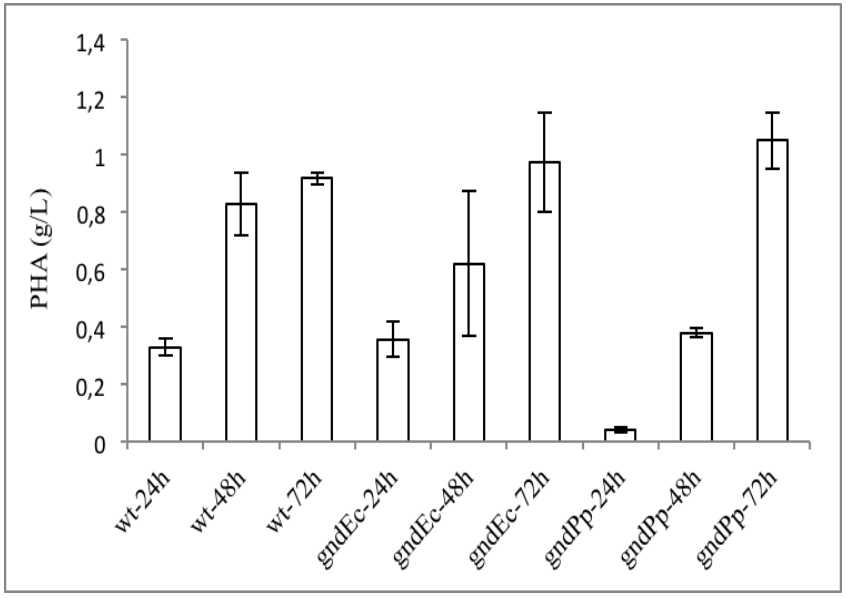

International Journal of Biological Macromolecules 163 (2020) 240–250

Contents lists available at ScienceDirect

International Journal of Biological Macromolecules

journal homepage: http://www.elsevier.com/locate/ijbiomac

The relevance of enzyme specificity for coenzymes and the presence of 6-phosphogluconate dehydrogenase for polyhydroxyalkanoates production in the metabolism of *Pseudomonas* sp. LFM046

Juliana Cardinali-Rezende [a,c,*], Alex Di Genova [b], Rafael A.T.P.S. Nahat [a], Alexander Steinbüchel [c,f], Marie-France Sagot [b], Rafael S. Costa [d,e], Henrique C. Oliveira [a], Marilda K. Taciro [a], Luiziana F. Silva [a], José Gregório C. Gomez [a,**]

Different enzymes specificity: NADH *versus* NADPH

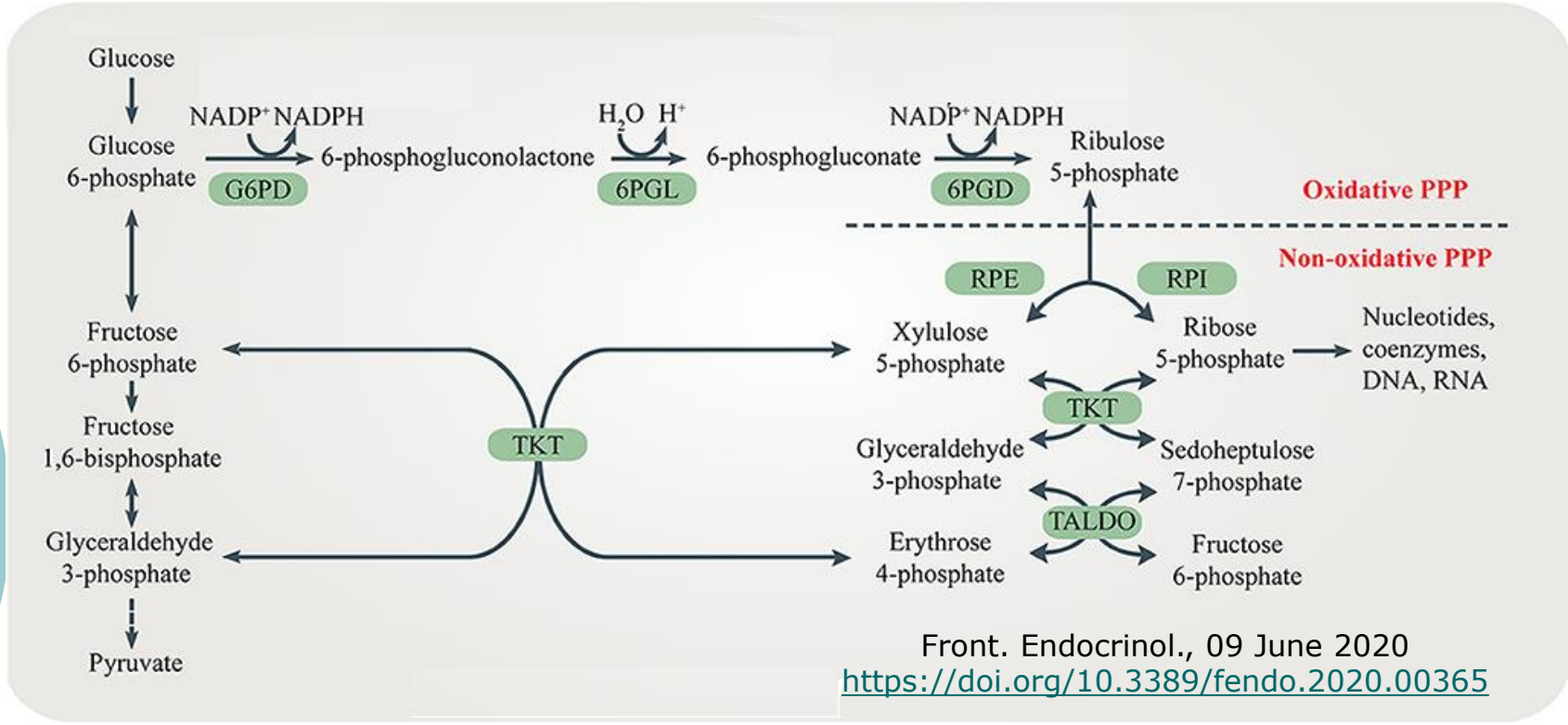

Front. Endocrinol., 09 June 2020
https://doi.org/10.3389/fendo.2020.00365

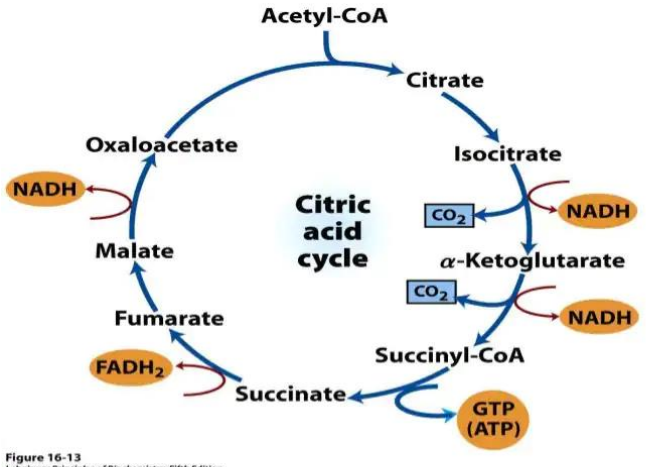

Figure 16-13
Lehninger Principles of Biochemistry, Fifth Edition
© 2008 W. H. Freeman and Company

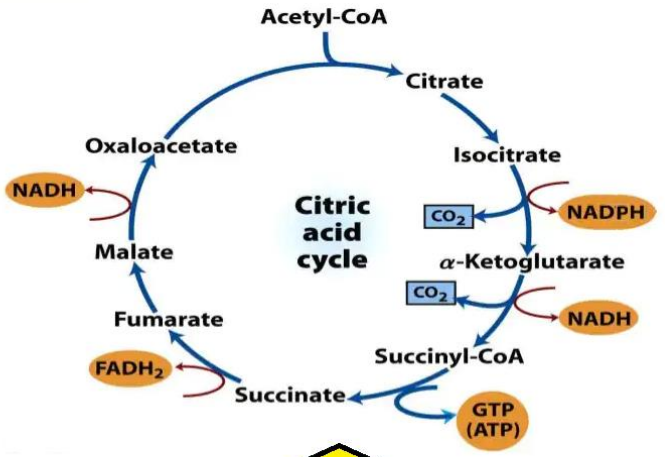

Most Bacteria

Different metabolic roles: NADH *versus* NADPH

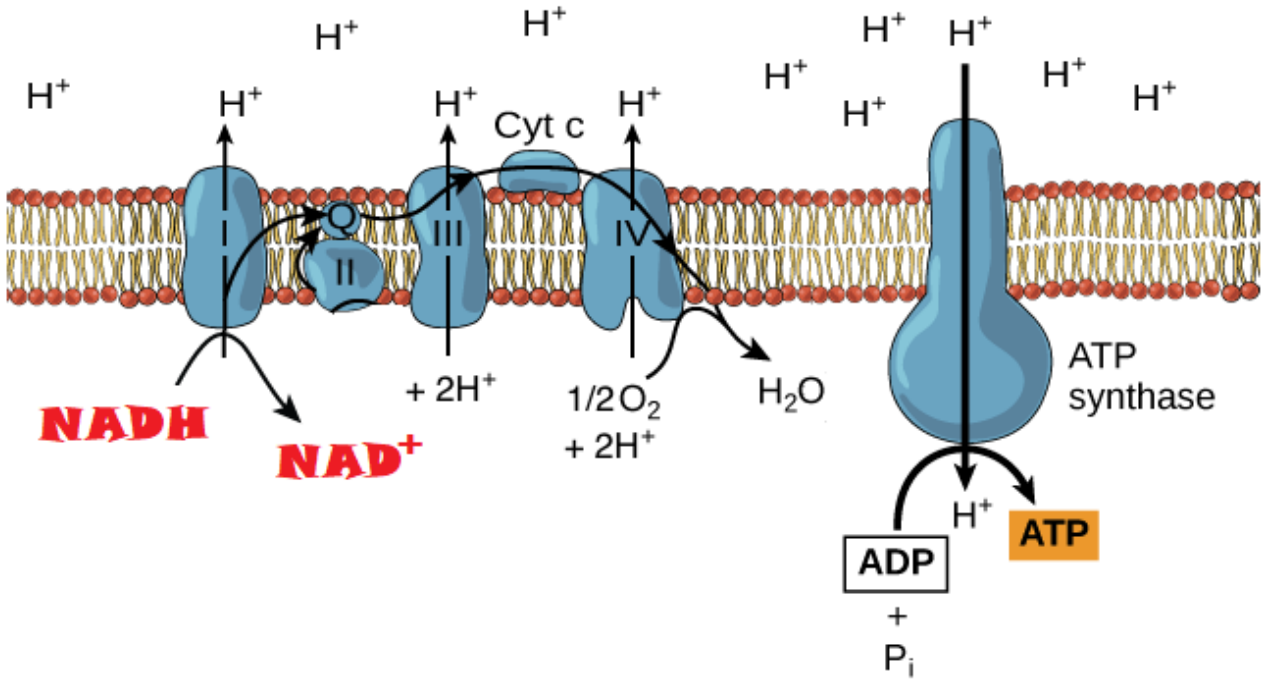

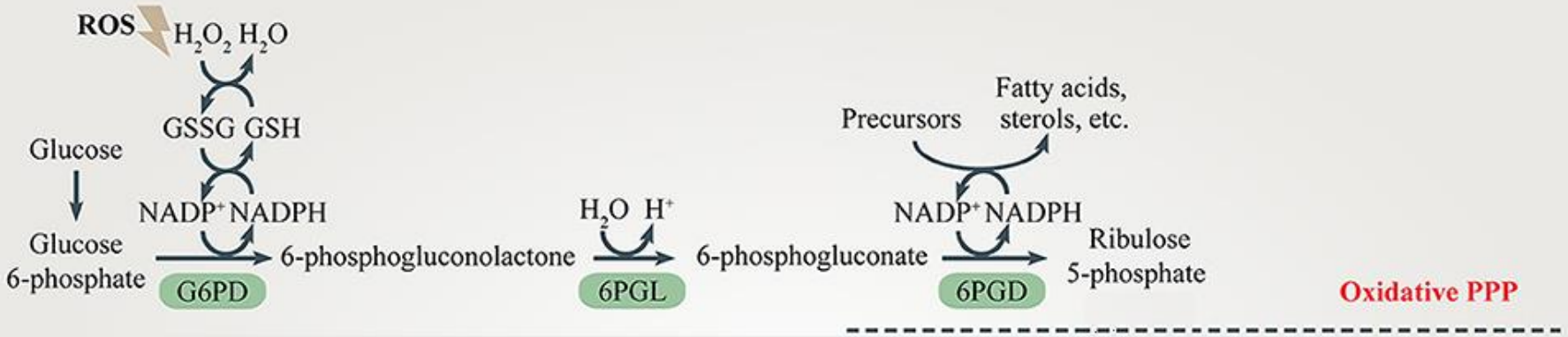

Front. Endocrinol., 09 June 2020
https://doi.org/10.3389/fendo.2020.00365

Imagem de autoria de Nara Guimarães

Flux distribution

Best labeling pattern

Genomic data
Enzymes activity

Experimental Data

ICB USP

^{13}C-MFA

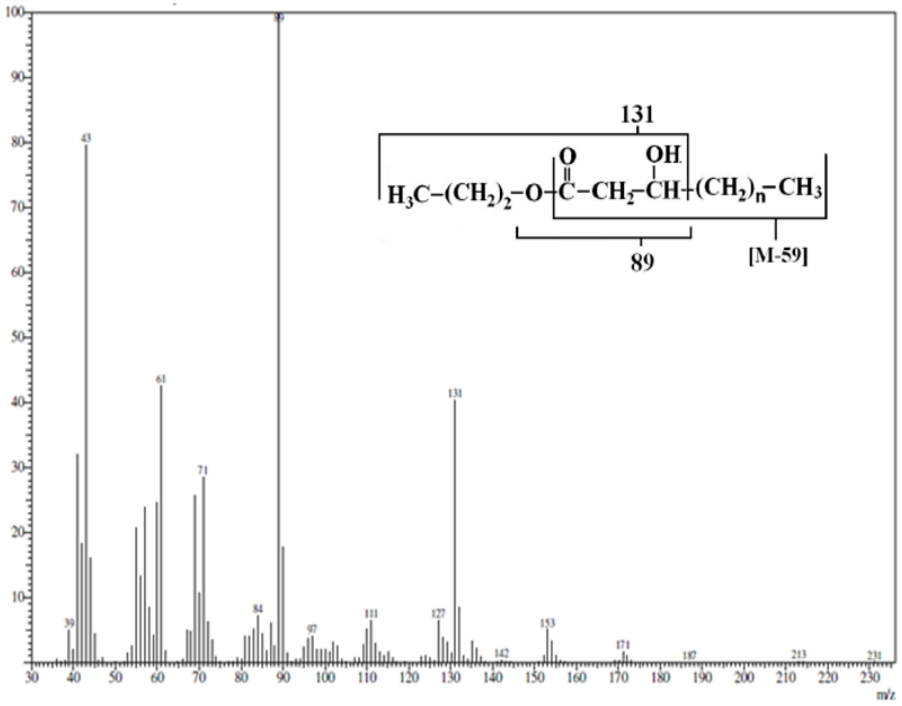
131
O
OH
$H_3C-(CH_2)_2-O-C-CH_2-CH-(CH_2)_n-CH_3$
89
[M-59]
m/z

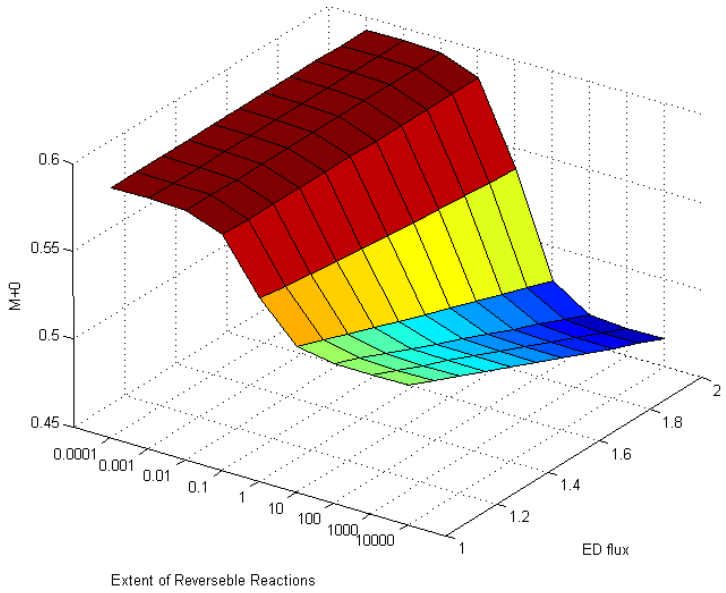
M+0
Extent of Reverseble Reactions
ED flux

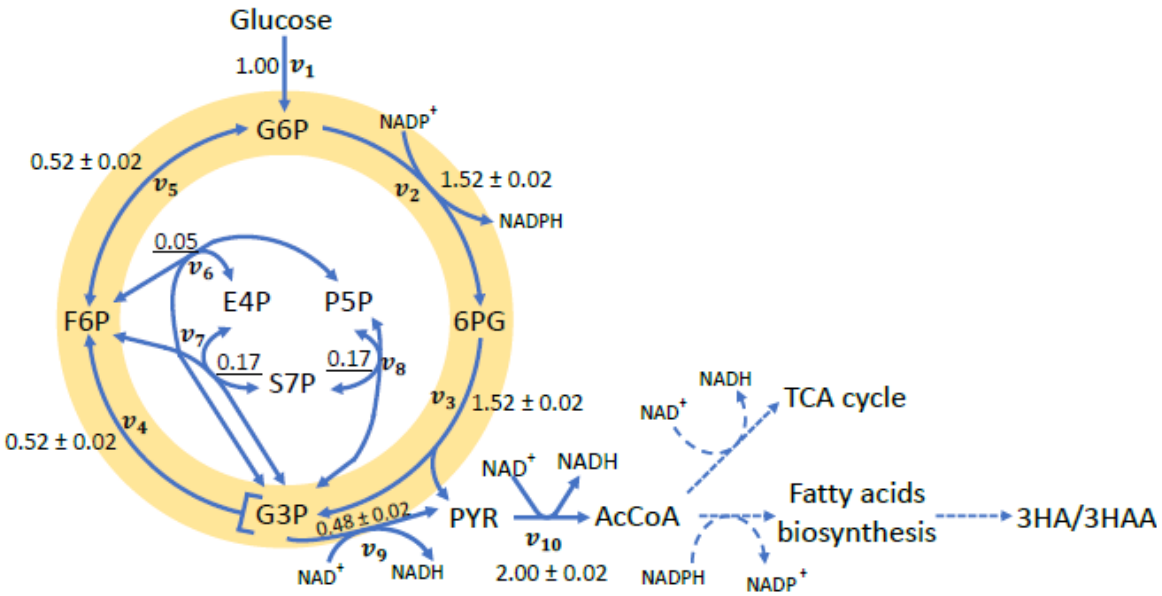
Glucose
1.00 v_1
G6P
NADP+
0.52 ± 0.02
v_5
v_2
1.52 ± 0.02
NADPH
0.05
v_6
E4P
P5P
F6P
v_7
6PG
0.17
S7P
0.17
v_8
v_3
1.52 ± 0.02
v_4
0.52 ± 0.02
NADH
NAD+
TCA cycle
NAD+
NADH
G3P
0.48 ± 0.02
PYR
AcCoA
Fatty acids
biosynthesis
3HA/3HAA
v_9
v_{10}
NAD+
NADH
2.00 ± 0.02
NADPH
NADP+

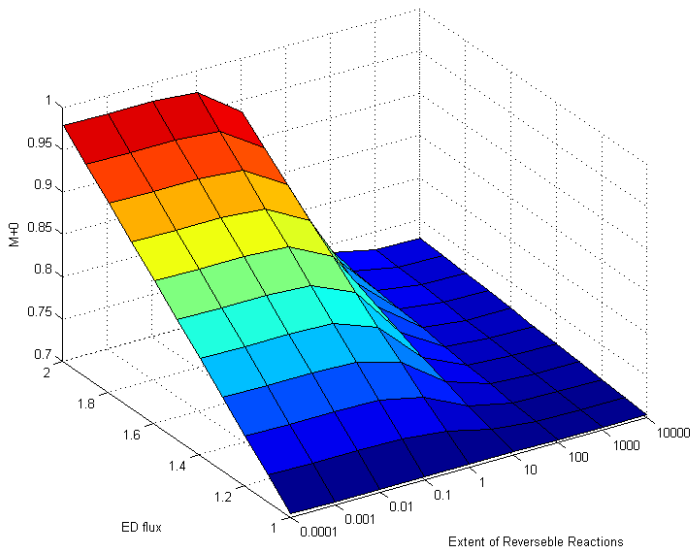
M+0
ED flux
Extent of Reverseble Reactions

PETROBRAS

DEPARTAMENTO DE MICROBIOLOGIA
UNIVERSIDADE DE SÃO PAULO

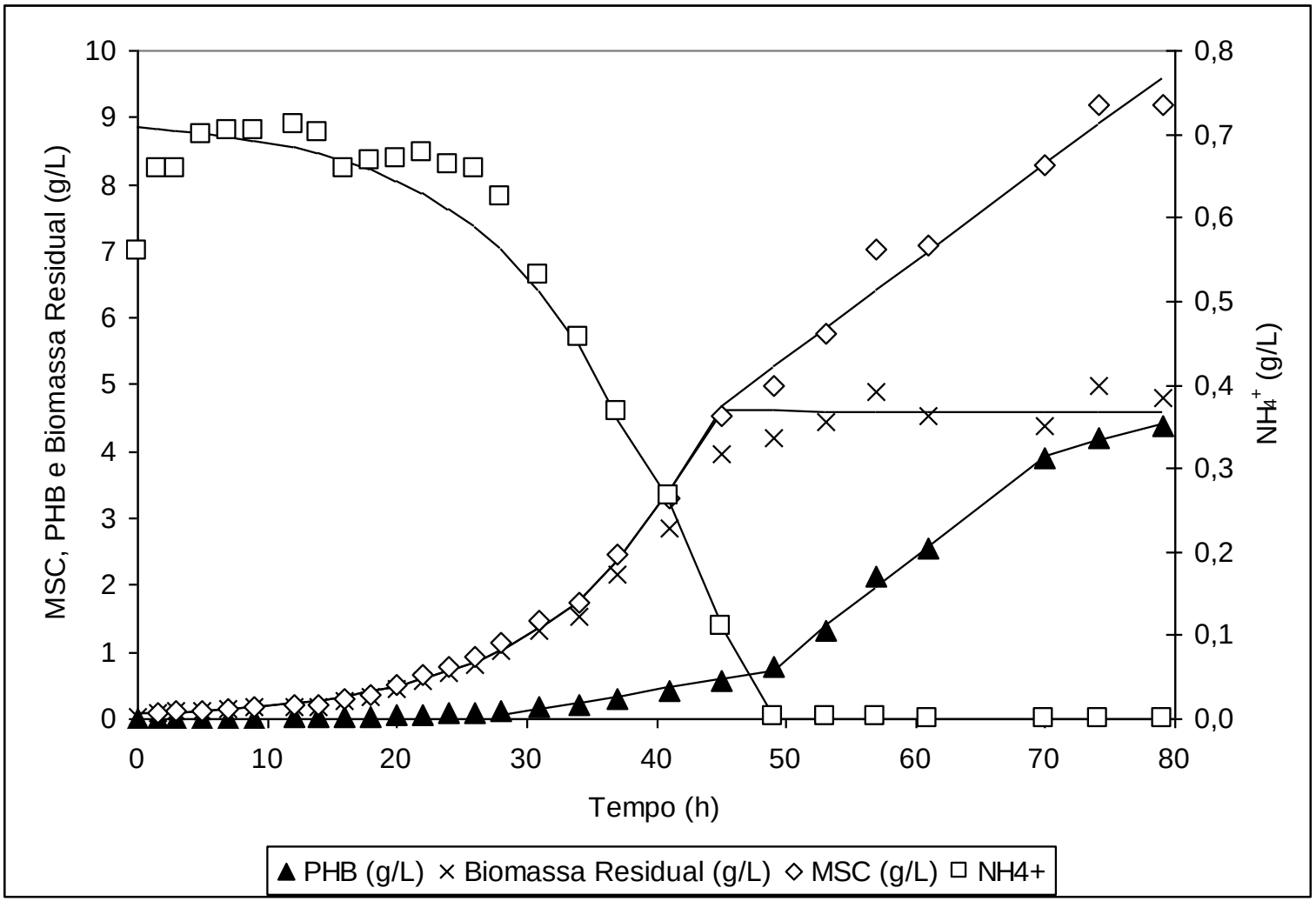

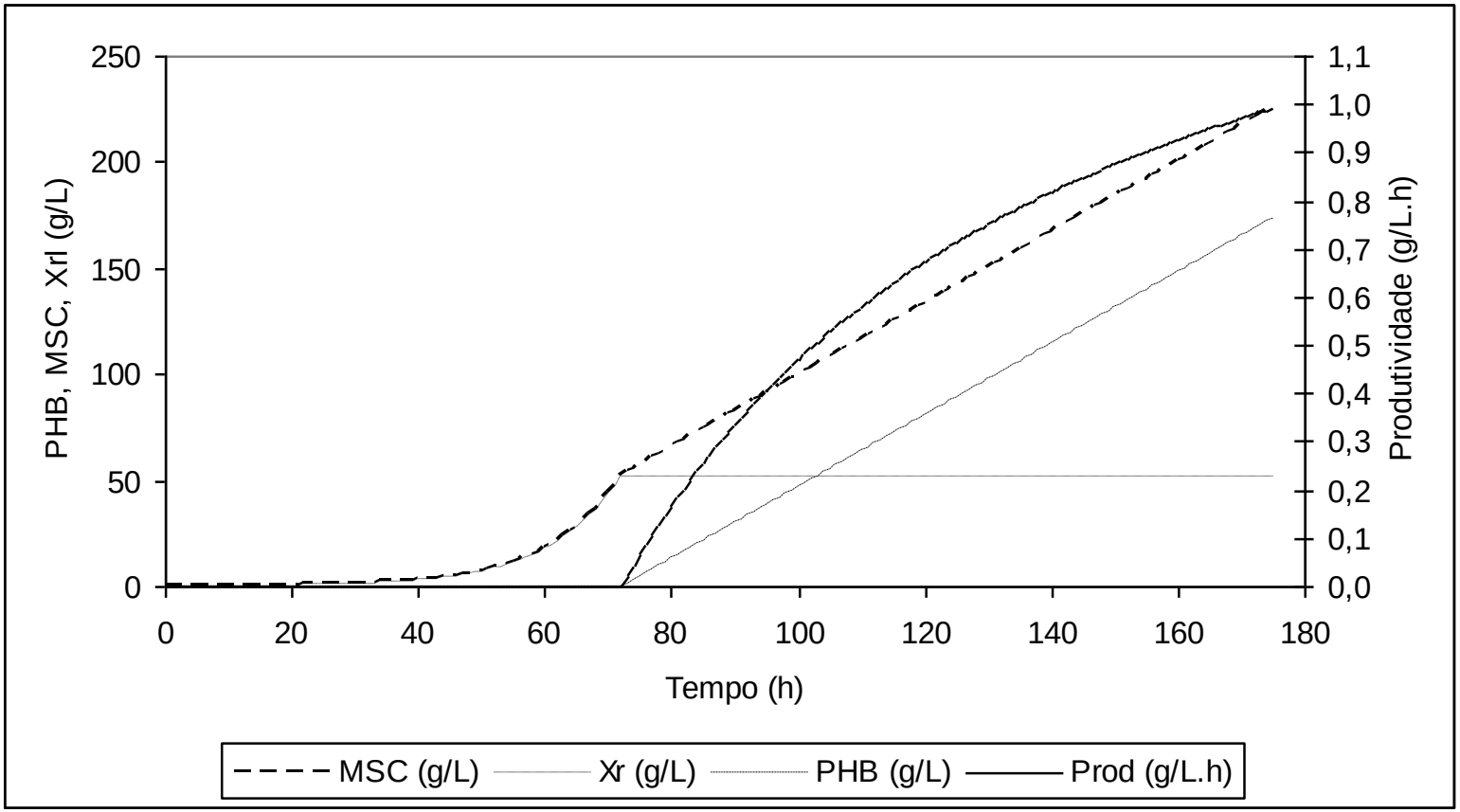

Figura 13. Simulação de processo de produção de P3HB para se atingir uma produtividade de aproximadamente 1 g/L.h, considerando μmax =0,09 h^{-1} e q_{P3HB} = 32,3 mg/g.h.

PETROBRAS

DEPARTAMENTO DE MICROBIOLOGIA
UNIVERSIDADE DE SÃO PAULO

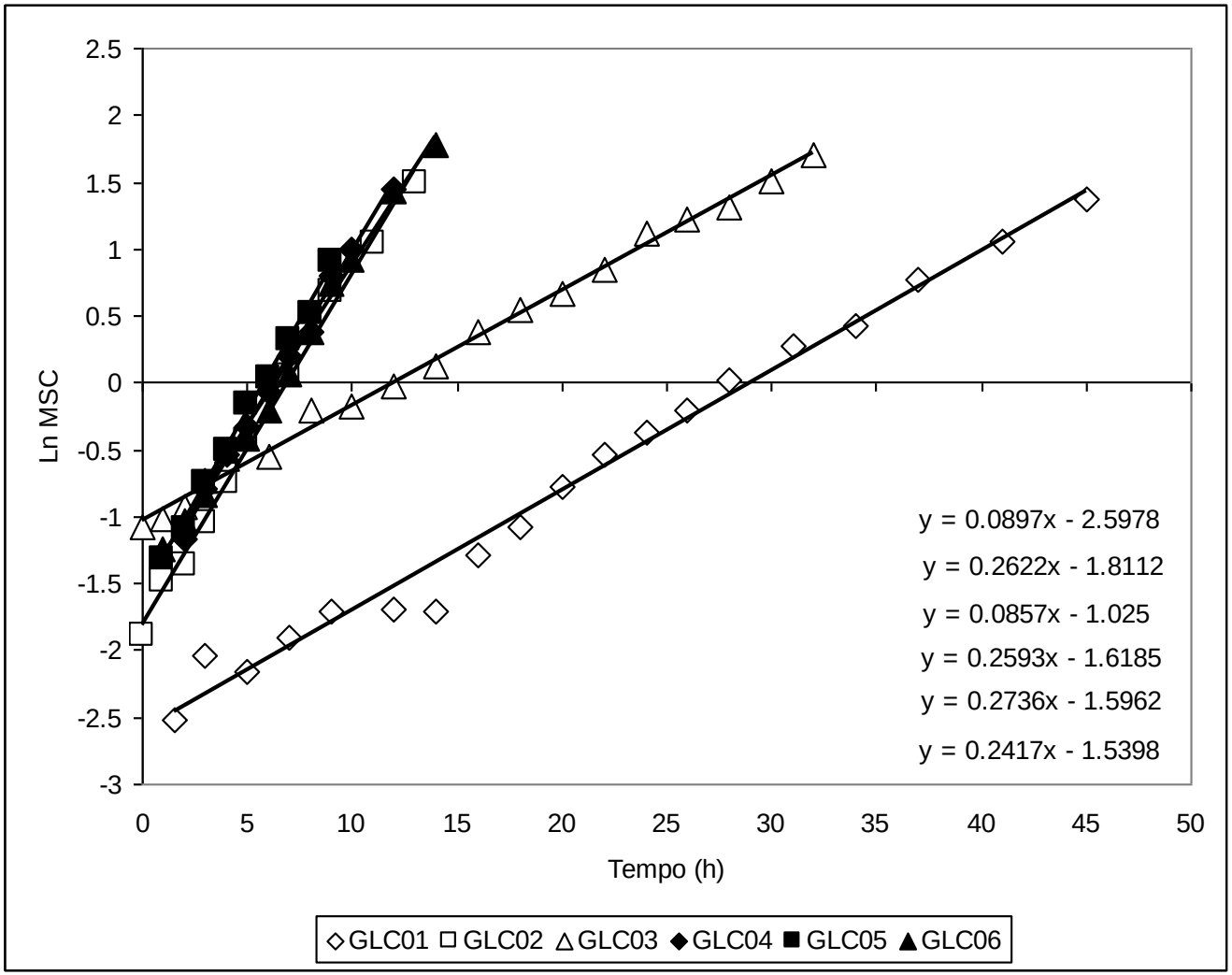

Poly-3-hydroxybutyrate in Recombinante *Escherichia coli*

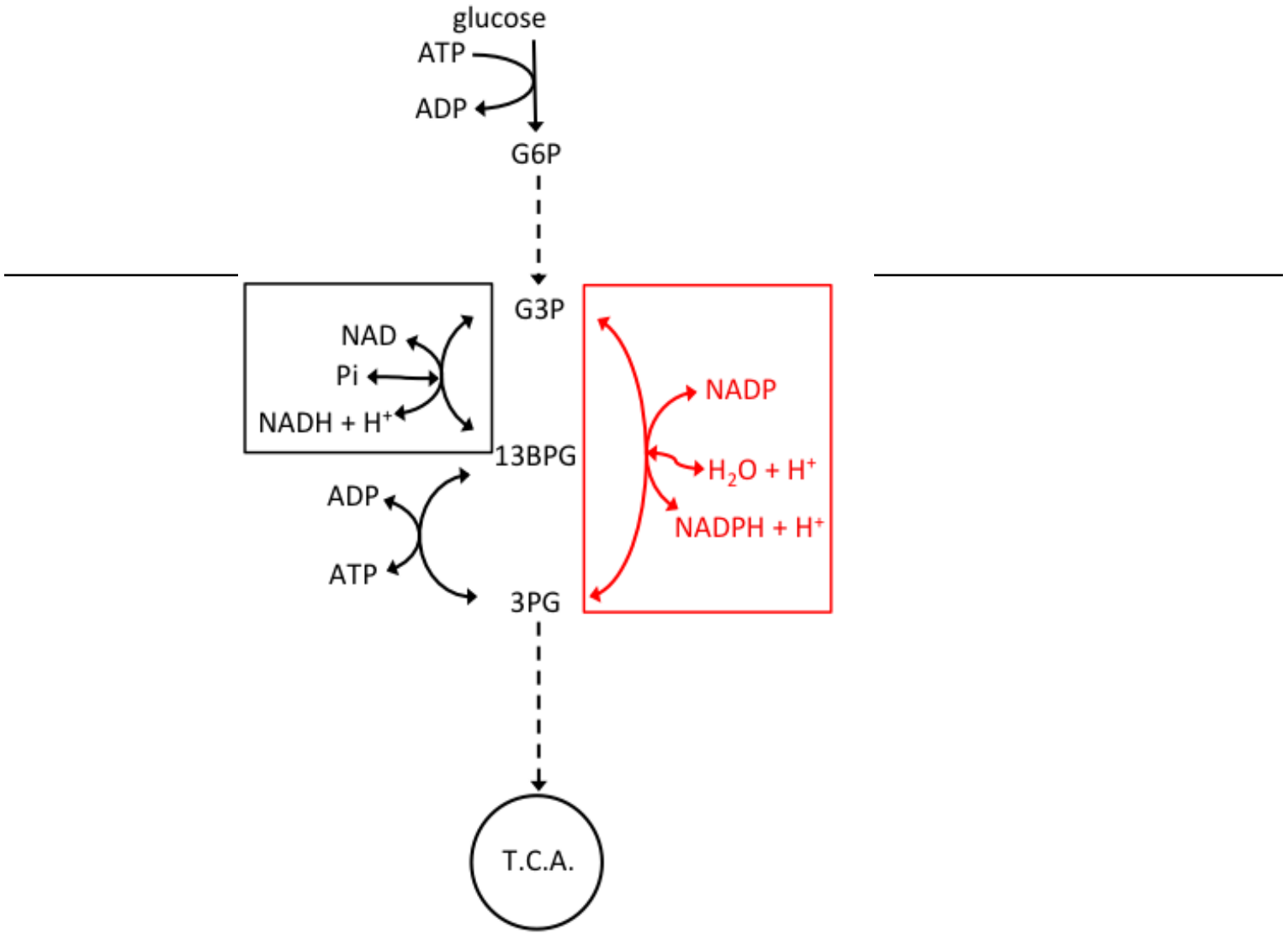
glucose
ATP
ADP
G6P
G3P
NAD
Pi
NADH + H+
NADP
H2O + H+
NADPH + H+
13BPG
ADP
ATP
3PG
T.C.A.

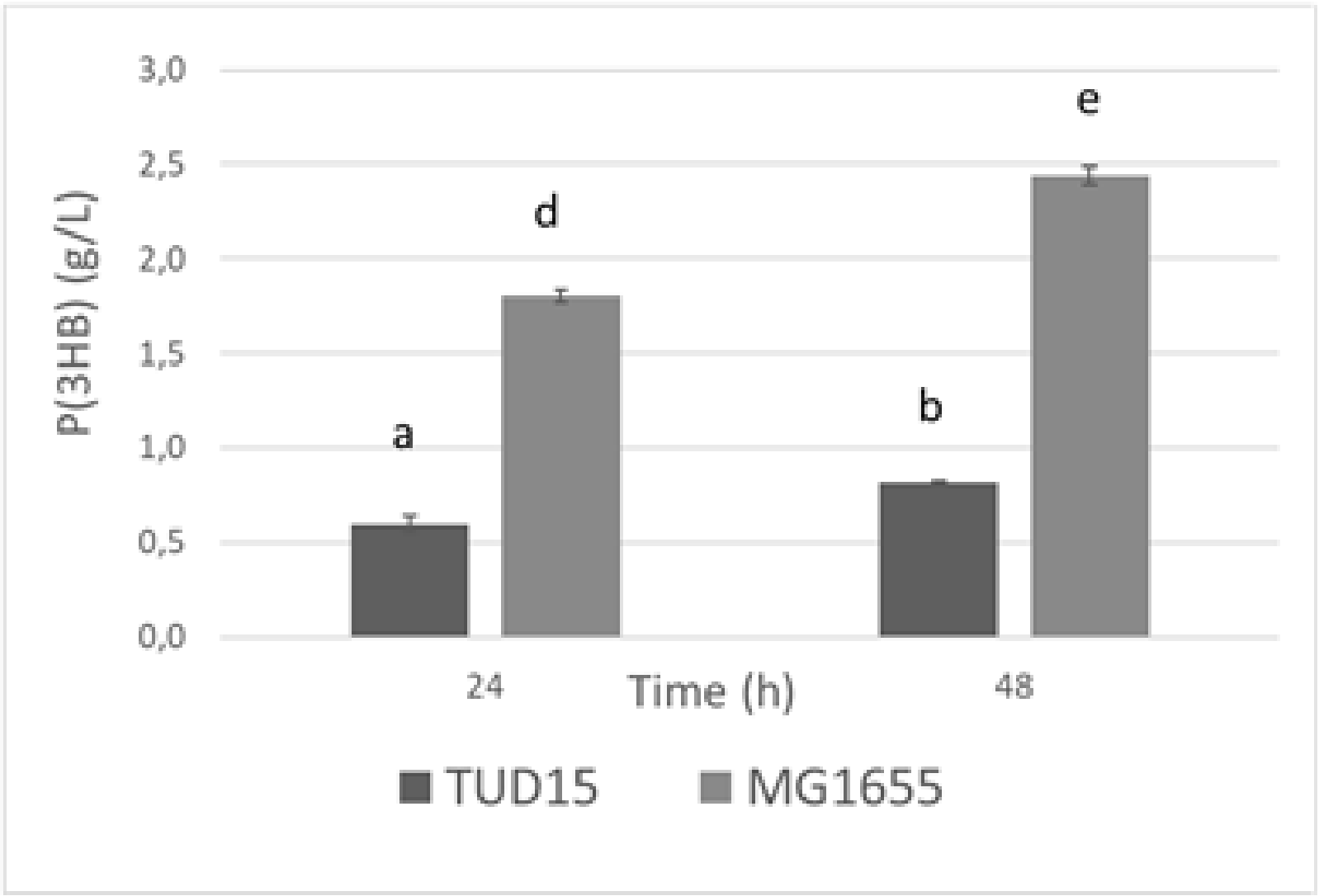

Figure 1. Production of P(3HB) by recombinant *E. coli* strains TUD15 and MG1655 (parental) harboring plasmid pBBR1MCS2:*phaCAB*. RCDW: residual cell dry biomass produced, CDW: total cell dry biomass produced.

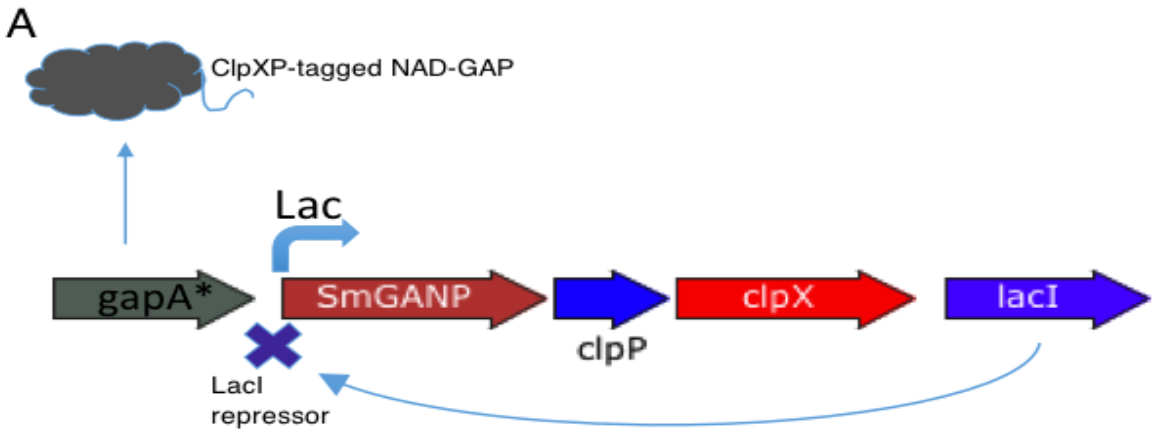
A
ClpXP-tagged NAD-GAP
Lac
gapA*
SmGANP
clpX
lacI
clpP
LacI
repressor

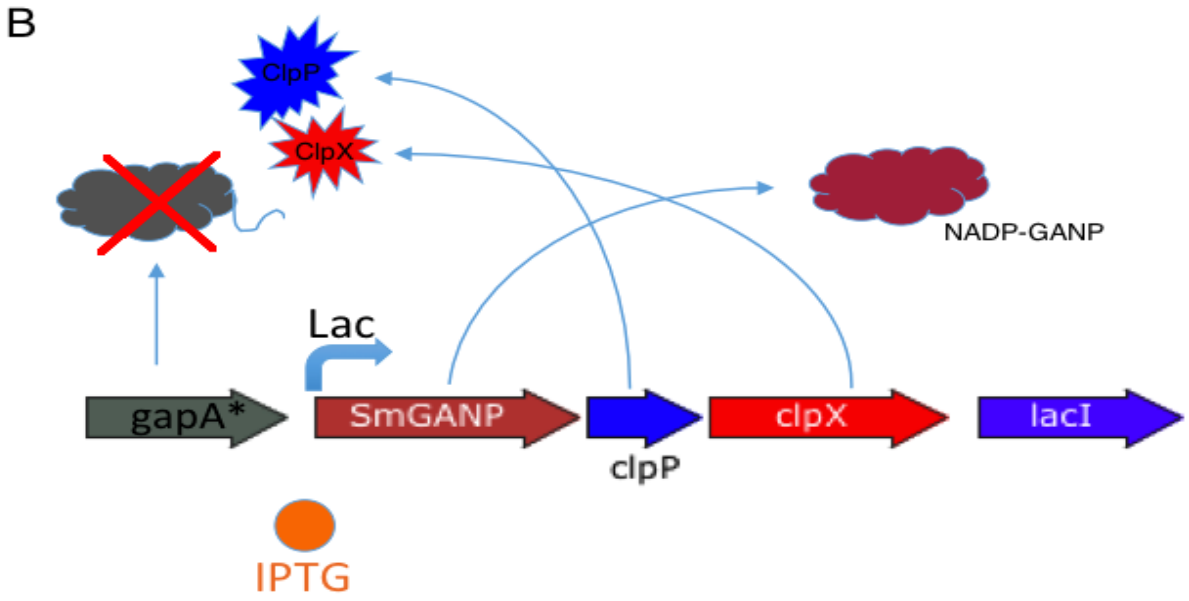
B
ClpP
ClpX
NADP-GANP
Lac
gapA*
SmGANP
clpX
lacI
clpP
IPTG

Table 2. Specific NAD-GAP and NADP-GANP activities measured in cellular extracts from the strains wild type (WT) and USP62. IPTG was added to the media at a final concentration of 1 mM. The cells were collected during the exponential growth phase. The values are average from three independent evaluations ± standard deviations.

strains	[a]NAD-GAP activity (mU/mg)	[b]NADP-GANP activity (mU/mg)
WT no IPTG	1325 ± 159	0
WT with IPTG	1346 ± 147	0
USP62 no IPTG	219 ± 21	0
USP62 with IPTG	727 ± 21	36 ± 8

[a] 50 mM sodium phosphate (pH 7.0), 20 mM sodium arsenate, 4 mM glyceraldehyde-3-phosphate and 2 mM NAD.

[b] 50 mM Tris (pH 8.5), 5 mM β-mercaptoethanol, 0.5 mM NADP, 1 mM glyceraldehyde-3-phosphate.

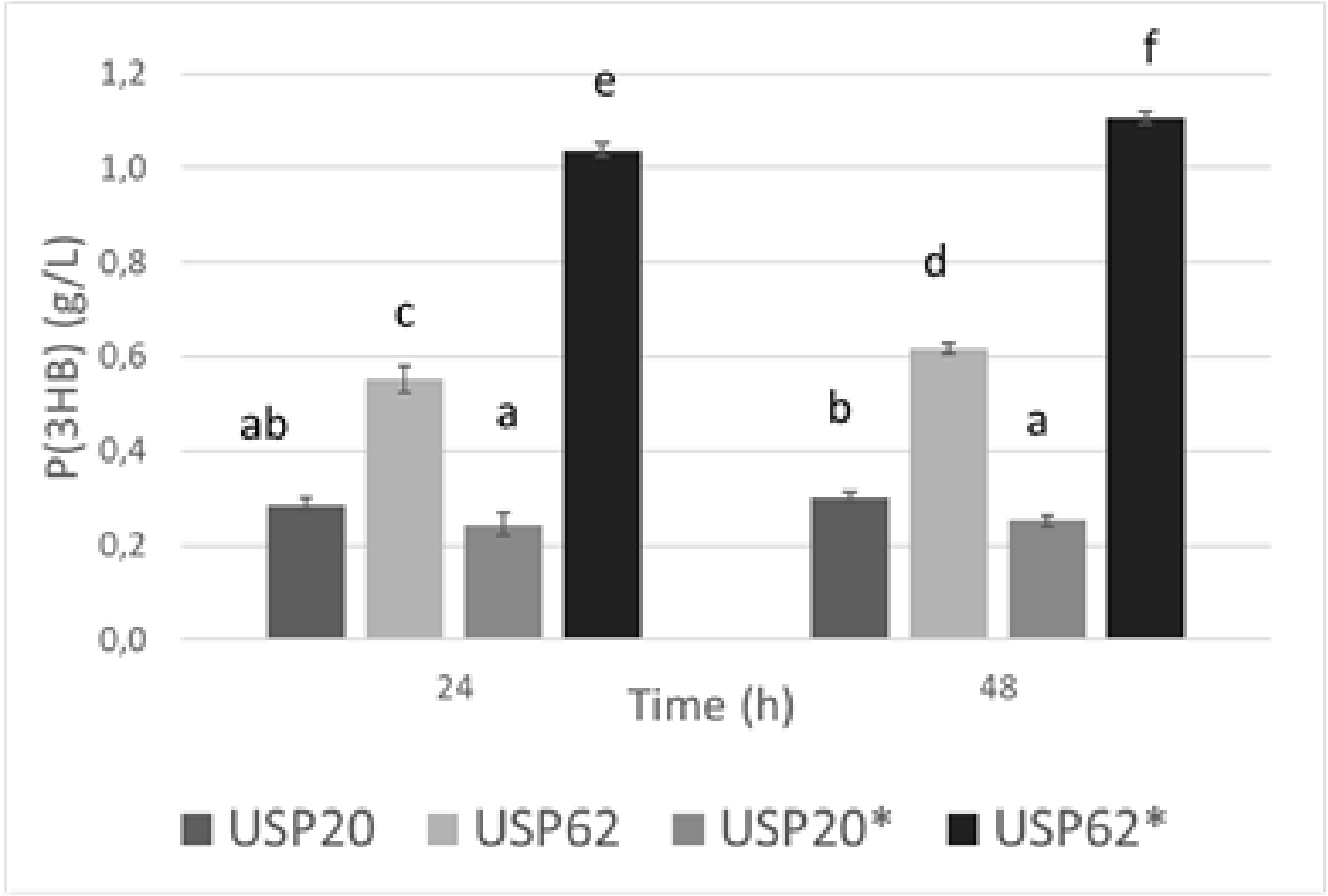

Figure 2. Production of P(3HB) by recombinant *E. coli* strains USP62 and USP20 (parental) harboring plasmid pBBR1MCS2:*phaCAB* with (*) and without the addition of IPTG. RCDW: residual cell dry biomass produced, CDW: total cell dry biomass produced.

1,3- propanediol production in Recombinante *Escherichia coli*

1,3-propanediol

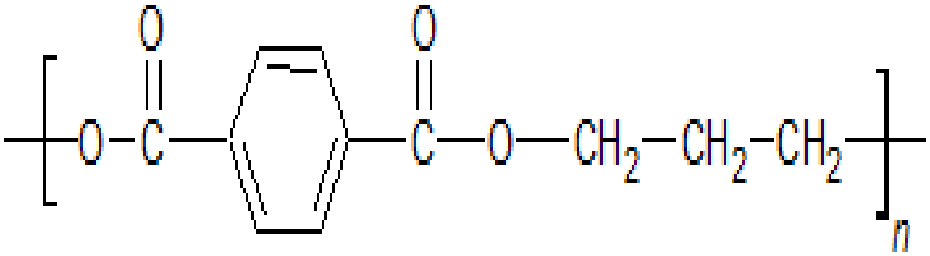

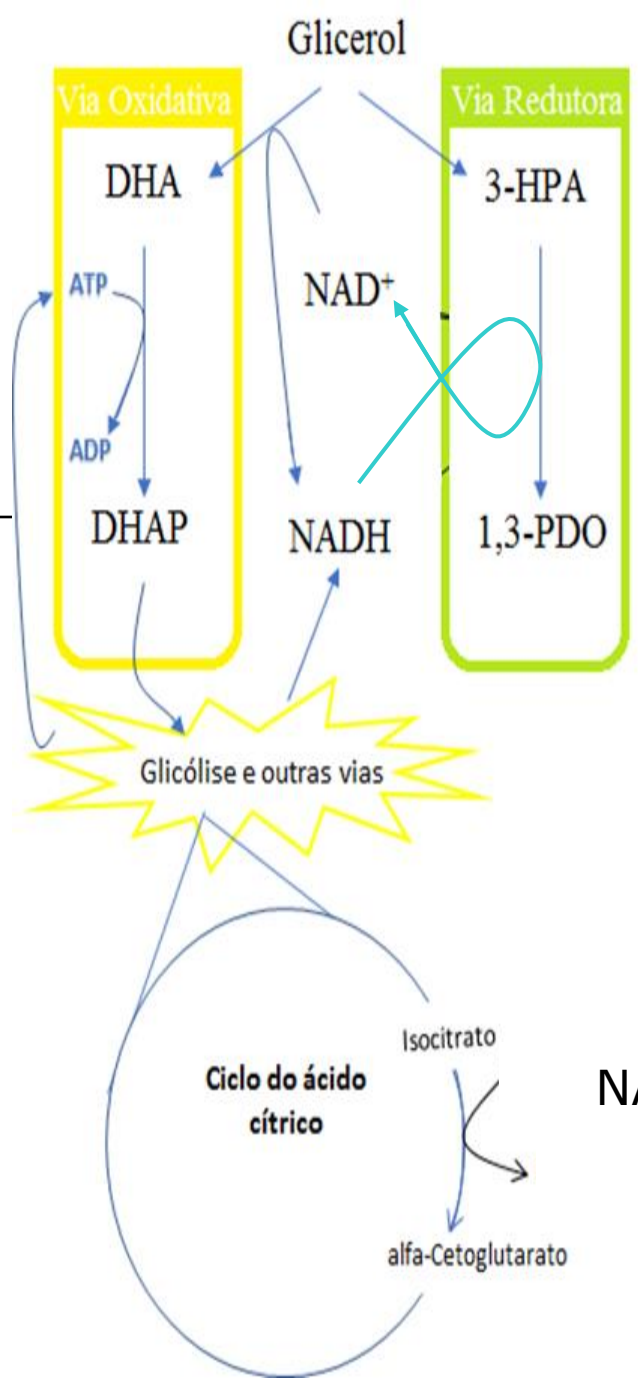
Glicerol
Via Oxidativa
Via Redutora
DHA
3-HPA
ATP
ADP
NAD+
DHAP
NADH
1,3-PDO
Glicólise e outras vias
Ciclo do ácido cítrico
Isocitrato
alfa-Cetoglutarato

NAD

NADH

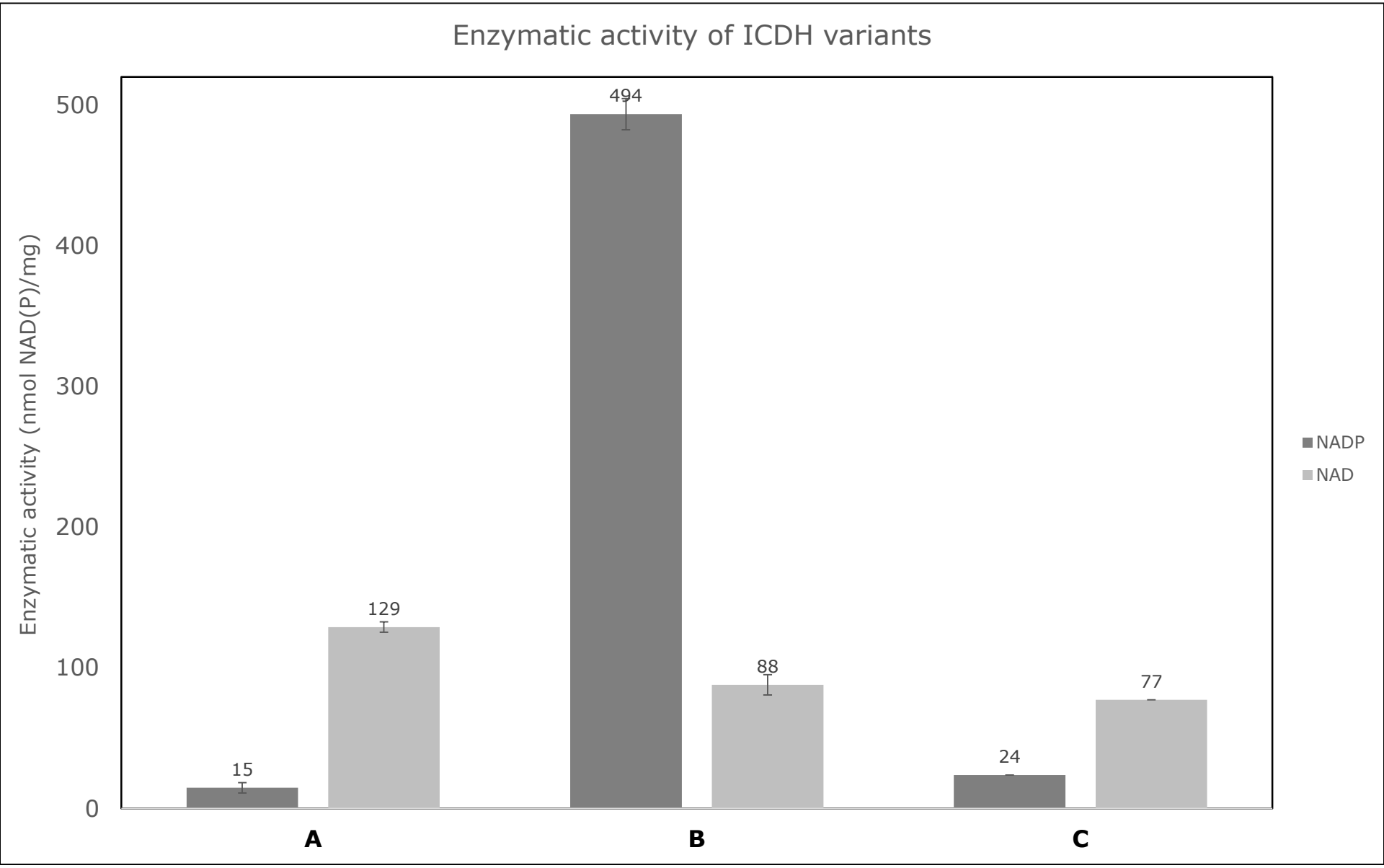

Figure 1:1 Enzymatic activity of ICDH variants. **A** = *E. coli* MG1655 Δ*icd* (pTrc99A::*icd*^{NAD}) + 20µM de IPTG; **B** = *E. coli* MG1655; **C** = *E. coli* MG1655 *icd*^{NAD}. (■) = with NADP; (■) = with NAD.

Prouction of 1,3-PDO by Recombinant *E. coli*

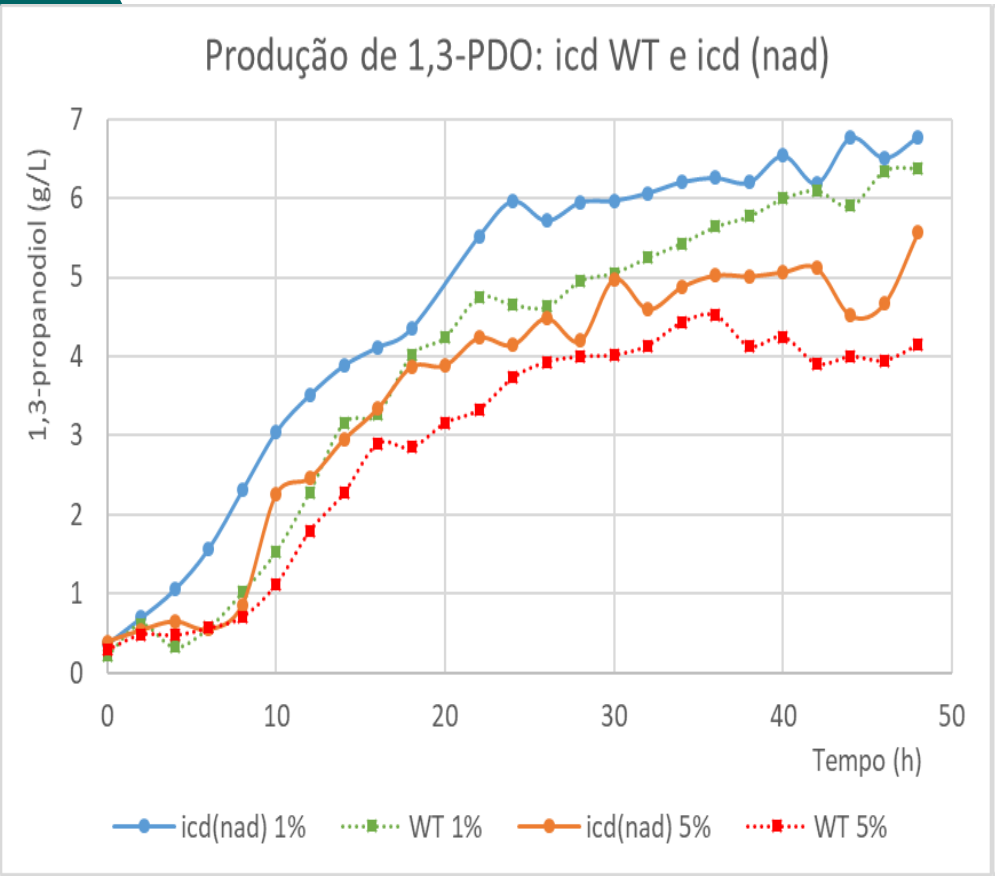

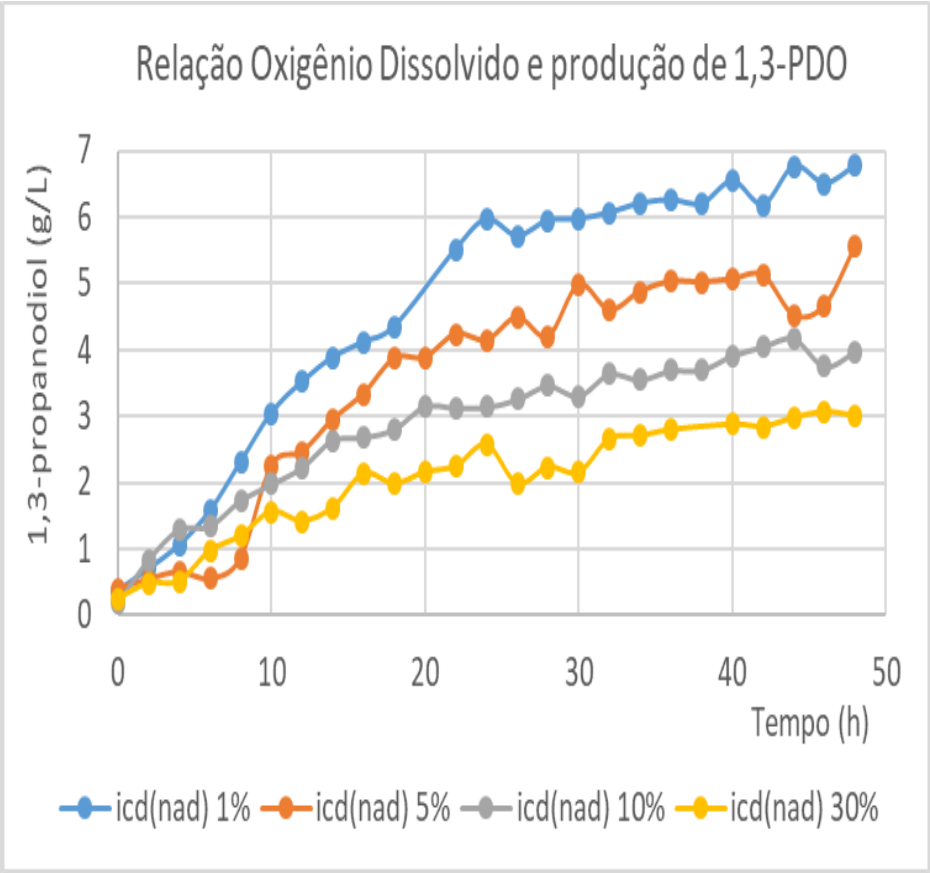

Trabalhos anteriores

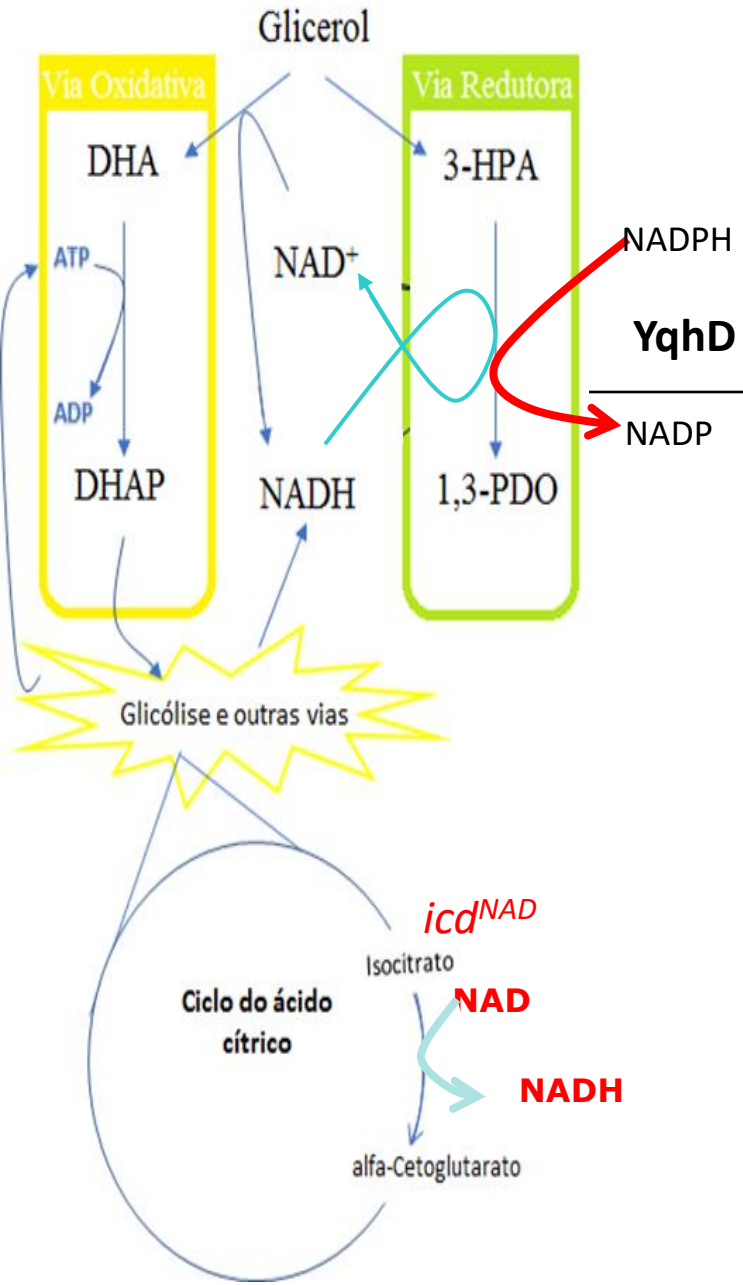

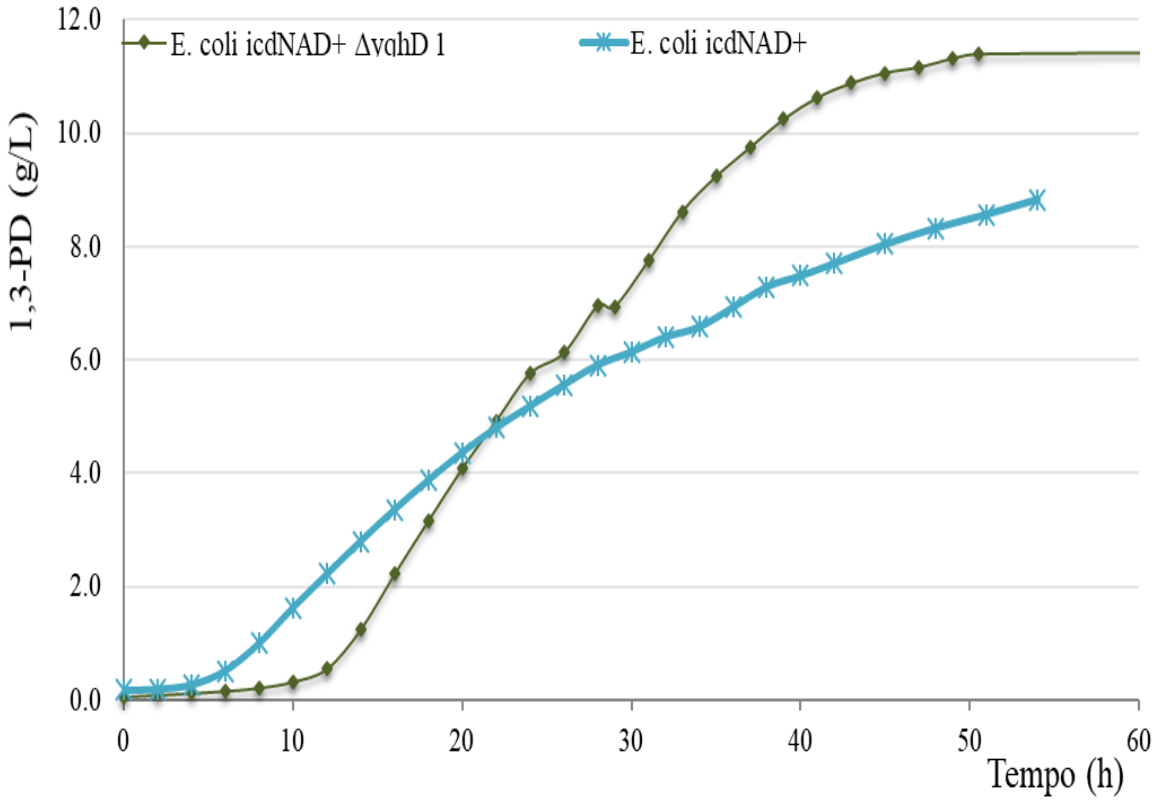

Global Transcription Machinery Engineering – Gtm Engineering

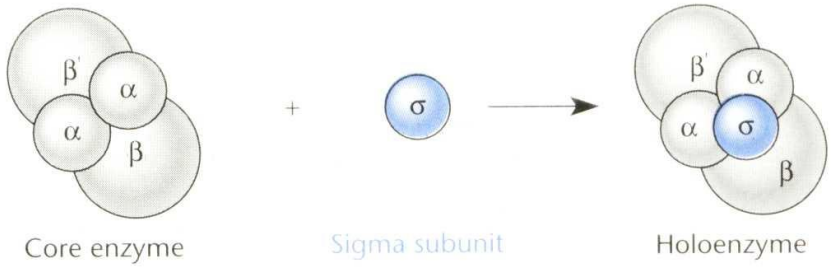

Figure 2.4 The composition of a typical bacterial RNA polymerase. The core enzyme contains two α subunits, a β subunit, and a β' subunit. The fifth subunit, the σ factor, cycles off after initiation of RNA synthesis.

Table 13.2 **Some of the Alternative Sigma (σ) Factors in Bacteria and Their Cognate Promoter Sequences**

σ Factor	Promoter Recognized	Genes Transcribed
σ^{70}	TTGACA-17bp-TATAAT	Many and diverse
σ^{32}	CNCTTGAA-14bp-CCCCATNT	Heat shock response
σ^{54}	CTGGNA-7bp-TTGCA	Many and diverse
σ^{28}	TAA-15bp-GCCGATAA	Chemotaxis, motility, flagellar components
σ^{29}	TTNAA-17bp-CATATT	Sporulation in *B. subtilis*[1]

[1]Several different sigma factors control different genes involved in sporulation in *B. subtilis*.

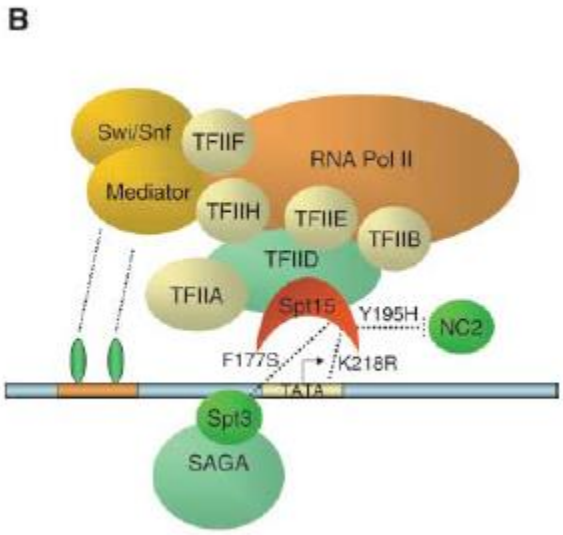

Global Transcription Machinery Engineering – gTME

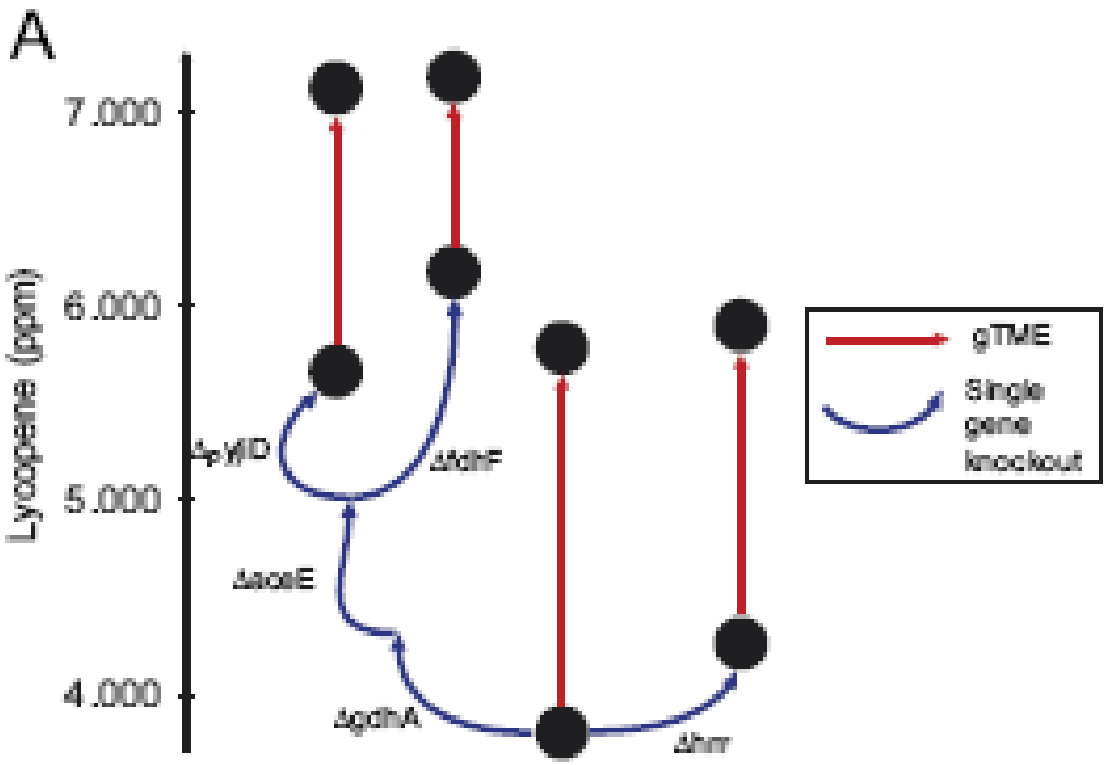

MAGE

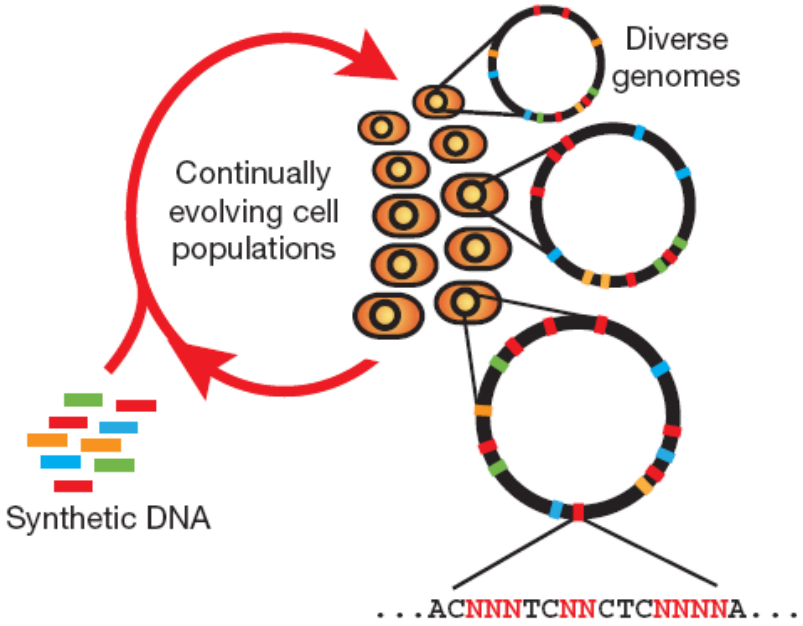

With the advent of next-generation fluorescent DNA sequencing[10], our ability to sequence genomes has greatly outpaced our ability to modify genomes. Existing cloning-based technologies are confined to serial and inefficient introduction of single DNA constructs into cells, requiring laborious and outdated genetic engineering techniques. Whereas *in vivo* methods such as recombination-based genetic engineering (recombineering) have enabled efficient modification of single genetic targets using single-stranded DNA (ssDNA)[11–14], no such attempts have been made to modify genomes on a large and parallel scale. MAGE provides a highly efficient, inexpensive and automated solution to simultaneously modify many genomic locations (for example, genes, regulatory regions) across different length scales, from the nucleotide to the genome level (Fig. 1).

Figure 1 | Multiplex automated genome engineering enables the rapid and continuous generation of sequence diversity at many targeted chromosomal locations across a large population of cells through the repeated introduction of synthetic DNA. Each cell contains a different set of mutations, producing a heterogeneous population of rich diversity (denoted by distinct chromosomes in different cells). Degenerate oligo pools that target specific genomic positions enable the generation of a diverse set of sequences at each chromosomal location.

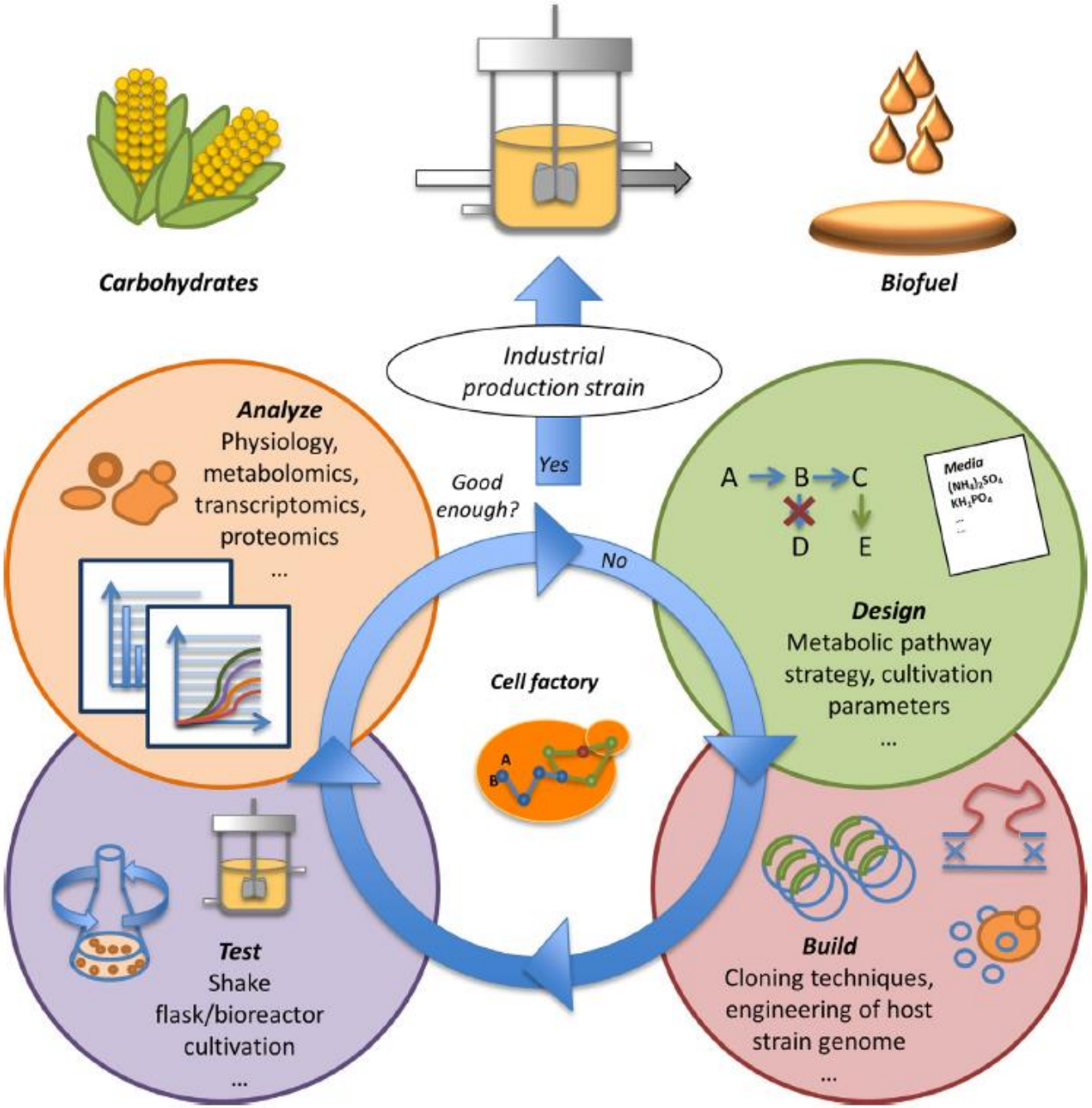

FIGURE 7.1 The iterative metabolic engineering cycle used to construct cell factories.

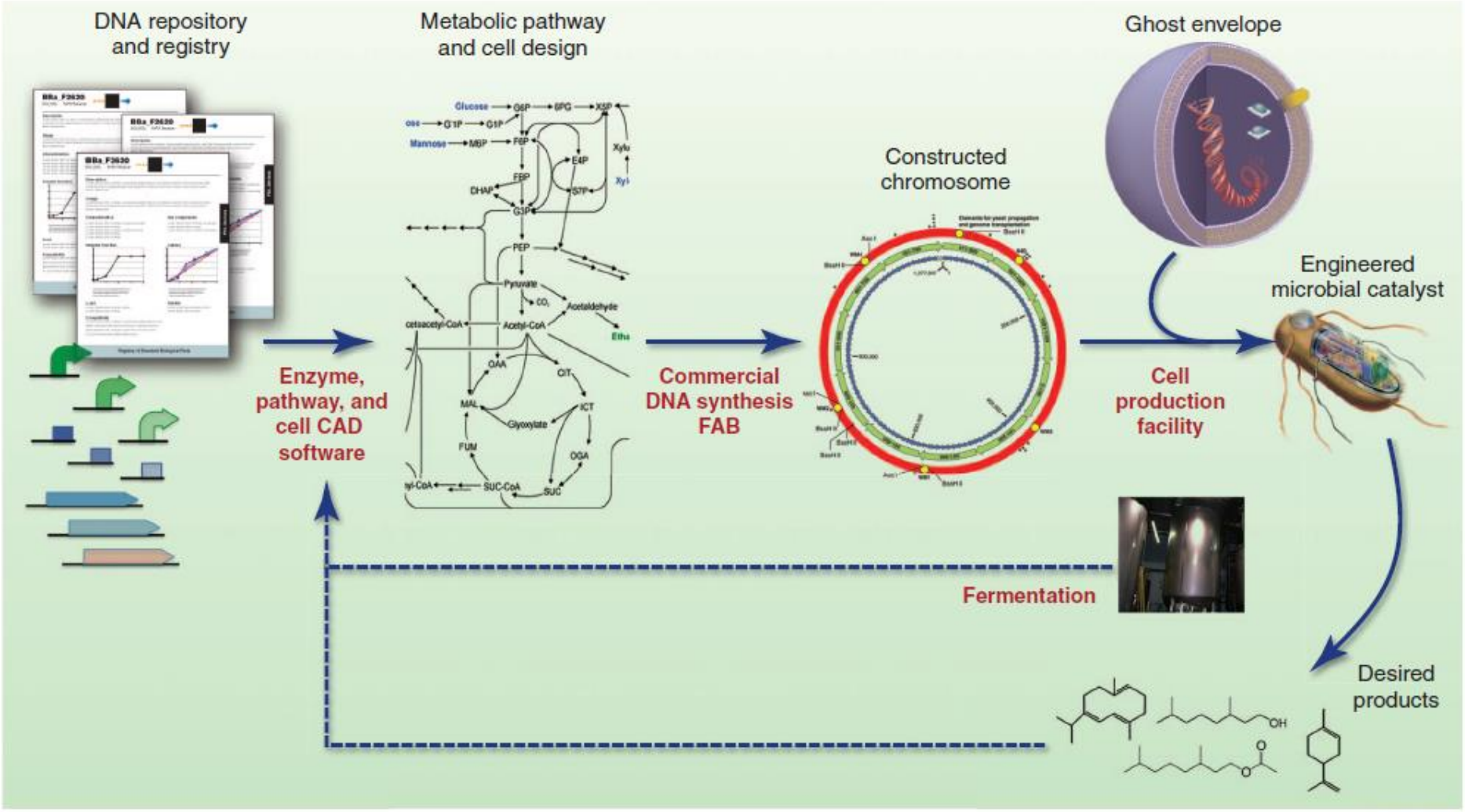

Fig. 3. The future of engineered biocatalysts. Pathways, enzymes, and genetic controls are designed from characteristics of parts (enzymes, promoters, etc.) by means of pathway and enzyme CAD software. The chromosomes encoding those elements are synthesized at a FAB and incorporated into a ghost envelope to obtain the new catalyst. The design of the engineered catalyst is influenced by the desired product and the production process.

Referências – Aula 1

•Carvalho, J.C.M. & Sato, S. 2001. Fementação descontínua alimentada. In Schimidell, W.; Lima, U.A.; Aquarone, E.; Borzani, W. **Biotecnologia Industrial.** Vol. 2 Engenharia Bioquímica. p. 205-218.

•Carvalho, J.C.M. & Sato, S. 2001. Fermentação descontínua. In Schimidell, W.; Lima, U.A.; Aquarone, E.; Borzani, W. **Biotecnologia Industrial.** Vol. 2 Engenharia Bioquímica. p. 193-204.

•Facciotti, M.C.R. 2001. Fermentação contínua. In Schimidell, W.; Lima, U.A.; Aquarone, E.; Borzani, W. **Biotecnologia Industrial.** Vol. 2 Engenharia Bioquímica. p. 223-246.

•Mukherjee, S.; Das, P.; Sem, R. 2006. Towards commercial production of microbial surfactants. **Trends n Biotechnology**, 24: 509-515.

•Riesenberg, D. & Guthke, R. 1999. High-cell-density cultivation of microorganisms. **Applied Microbiology and Biotechnology**, 51: 422-430.

•Schimidell, W. & Facciotti, MC.R. 2001. Biorreatores e processos fermentativos. In Schimidell, W.; Lima, U.A.; Aquarone, E.; Borzani, W. **Biotecnologia Industrial.** Vol. 2 Engenharia Bioquímica. p. 179-192.

•Schimidell, W. 2001 Microrganismos e meios de cultura para utilização industrial. In Schimidell, W.; Lima, U.A.; Aquarone, E.; Borzani, W. **Biotecnologia Industrial.** Vol. 2 Engenharia Bioquímica. p. 5-18.

•Zhang, J. & Greasham, R. 1999. Chemically defined media for commercial fermentations. **Applied Microbiology and Biotechnology**, 51: 407-421.

Referências Aula 2

1. Nielsen, J. 2003. It is all about metabolic fluxes. Journal of Bacteriology, 185: 7031-7035.
2. Nielsen, J. & Jewett, M.C. 2008. Impact of system biology on metabolic engineering of Saccharomyces cerevisiae. FEMS Yeast Research, XX: XXXX-XXXX.
3. Tyo, K.E.; Alper, H.S. & Stephanopoulos, G.N. 2007. Expanding the metabolic engineering toolbox: more options to engineer cells. Trends in Biotechnology, 25: 132-137.
4. Keasling, J. 2010. Manufacturing molecules through metabolic engineering. Science, 330: 1355-1358.
5. Gomez, J.G.C. Engenharia Metabólica, Biologia de Sistemas e o desenvolvimento de processos biotecnológicos microbianos. REBEQ, Julho 2016.